Deep–Sea Research I 213 (2024) 104404

Contents lists available at ScienceDirect

Deep-Sea Research Part I

journal homepage: www.elsevier.com/locate/dsri

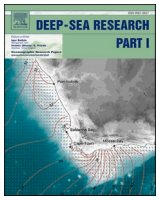

Mesoscale ocean eddies determine dispersal and connectivity of corals at the RMS *Titanic* wreck site

Tobias Schulzki [a,*], Lea-Anne Henry [b], J. Murray Roberts [b], Maria Rakka [c,d], Steve W. Ross [e], Arne Biastoch [a,f]

[a] GEOMAR Helmholtz Centre for Ocean Research, Kiel, Germany
[b] School of GeoSciences, University of Edinburgh, Edinburgh, UK
[c] Institute of Marine Sciences - Okeanos, University of the Azores, Horta, Portugal
[d] Oceanography Department, Dalhousie University, Halifax, NS, Canada
[e] Center for Marine Science, University of North Carolina at Wilmington, Wilmington, NC, United States
[f] Kiel University, Kiel, Germany

ARTICLE INFO

Keywords:
RMS Titanic
Deep-sea octocorals
Lagrangian modeling
Biophysical connectivity
Mesoscale eddies
Chrysogorgia cf. agassizii

ABSTRACT

The sinking of the RMS *Titanic* on 15 April 1912 remains one of most iconic maritime disasters in history. Today, the wreck site lies in waters 3800 m deep approximately 690 km south southeast of Newfoundland, Atlantic Canada. The wreck and debris field have been colonized by many marine organisms including the octocoral *Chrysogorgia agassizii*. Because of the rapid deterioration of the *Titanic* and the vulnerability of natural deep-sea coral populations to environmental changes, it is vital to understand the role the *Titanic* as well as other such structures could play in connecting ecosystems along the North American slope. Based on Lagrangian experiments with more than one million virtual particles and different scenarios for larval behavior, given the uncertainties around the biology of *chrysogorgiids*, the dispersal of larvae spawned at the *Titanic* wreck is studied in a high-resolution numerical ocean model. While the large-scale bathymetry shields the *Titanic* from a strong mean flow, mesoscale ocean eddies can considerably affect the deep circulation and cause a significant speed up, or also a reversal, of the circulation. As a consequence, the position of upper and mid-ocean eddies in the model largely controls the direction and distance of larval dispersal, with the impact of eddies outweighing the importance of active larval swimming in our experiments. Although dependent on larval buoyancy and longevity, we find that the *Titanic* could be reached by larvae spawned on the upper slope east of the Grand Banks. Therefore, the *Titanic* could act as a stepping stone connecting the upper to the deep continental slope off Newfoundland. From the *Titanic*, larvae then spread into deep Canadian waters and areas beyond national jurisdiction.

1. Introduction

The sinking of the RMS *Titanic* on 15 April 1912 was one of the deadliest and most iconic maritime disasters in history. More than 1500 people lost their lives, and today the wreckage site lies in waters 3800 m deep approximately 690 km south southeast of Newfoundland in Atlantic Canada. The wreck site was discovered in 1985, but it was not until 2012 that the site could be safeguarded by the UNESCO Convention on the Protection of Underwater Cultural Heritage, albeit this does not afford full site protection (Martin, 2018). The case could be made that the *Titanic* and its debris field are resting on the seafloor (the "Area") and more specifically in Areas Beyond National Jurisdiction (ABNJ), but equally a case could be made that they actually rest on the outer edge of Canada's continental margin (Aznar and Varmer, 2013). To further safeguard its protection and address other issues such as looting and unwanted salvage, a multilateral "Agreement Concerning the Shipwrecked Vessel RMS *Titanic*" came into force in 2019 after negotiations between Canada, the United Kingdom, France, and the United States.

Besides its monumental cultural legacy, the wreck has laid in place for more than a century now, acting as a hard substratum for benthic settlement amongst mostly soft-bottom seafloor with the occasional

* Corresponding author. Geomar Helmholtz Centre for Ocean Research, Düsternbrooker Weg 20, Kiel, Germany.
E-mail address: tschulzki@geomar.de (T. Schulzki).

https://doi.org/10.1016/j.dsr.2024.104404
Received 6 February 2023; Received in revised form 20 June 2024; Accepted 3 October 2024
Available online 3 October 2024

rocky outcrop. The wreck and its associated debris field of anthropogenic structures now support biologically diverse epifaunal assemblages, including numerous cold-water corals and sponges. The role that shipwrecks play in facilitating ecological connectivity and the role of underwater cultural heritage more generally have gained research interest over the last decade, (e.g. Meyer-Kaiser and Mires, 2022). Studies can identify important sources, sinks and the corridors used by organisms for dispersal: this knowledge can inform policy decisions about area-based management tools such as marine protected areas (MPAs) to halt or reverse loss of biodiversity and optimize ecosystem services such as fisheries benefits (Fontoura et al., 2022). As isolated but abundant and globally distributed habitats on the seafloor, shipwrecks effectively reduce the distances that organisms must disperse from, or travel to, in order to be connected to upstream and downstream populations and habitats (Gravina et al., 2021; Hamdan et al., 2021; Paxton et al., 2019; Ross et al., 2016). The *Titanic* is now rapidly degrading by corrosion (Salazar and Little, 2017), much of which is mediated by microbial communities leaching iron from the structure in an oxidative environment (Cullimore and Johnston, 2008). As a consequence, the *Titanic*'s potential impact on ecosystem connectivity may be lost in the future.

In this study, we focus on one of the most commonly encountered species found at the wreck site, the octocoral *Chrysogorgia agassizii*, and use it as a case study to investigate dispersal from and to the *Titanic* and the wreck's role in promoting wider connectivity. The genus *Chrysogorgia* is an abundant and diverse octocoral taxon with at least 68 nominal species and worldwide distribution in waters 31–4492 m deep into the abyss (Cairns, 2001; Untiedt et al., 2021; Baena et al., 2024). Species of this genus are commonly encountered on the continental slope and on seamounts of the Northwest Atlantic, as well as in proximity to the wreck site (Baker et al., 2012; Lecours et al., 2020; Meredyk et al., 2020). It has been hypothesized that shallow water *Chrysogorgia* spp. evolved from deep-water ancestors (Pante et al., 2012), and large biogeographic ranges in the genus suggest their larvae are capable of long-range dispersal.

Chrysogorgia agassizii has been commonly documented on the *Titanic* wreck based on visual identifications, including a quite prominent occurrence on the upper rail of the ship's bow (Vinogradov, 2000). While Molodtsova et al. (2008) noted this could be *C. campanula*, we retain the original identification of *C. agassizii* until an integrated morphological and genetic study can be conducted. Repeat surveys allowed detailed investigation of coral growth rates, showing relatively fast growth for a deep-sea coral (approximately 1 cm/year linear extension; Vinogradov, 2000). Recent accounts at the wreck site during 2021 and 2022 no longer document *C. agassizii* in the same position on the upper rail of the bow, but the species remains a common member of *Titanic*'s sessile marine growth community on the ship's bow and elsewhere (SWR pers. obs.; Fig. 1), and is thought to have high potential for widespread dispersal (Pante et al., 2012). Thus, its occurrence on the wreck offers an opportunity to use this species as a model system to explore how the natural heritage of the *Titanic* may confer a legacy connecting to marine ecosystems further afield.

Since there is limited life history information for most chrysogorgiids, including the two species above, the exercise undertaken in this paper remains relevant, especially as related to the genus *Chrysogorgia*. Although we focus on the connectivity of the *Titanic* to known occurrences of *C. agassizii*, the results are also valid for other species suspected to have long-range dispersal capabilities.

In order to investigate population connectivity of cold-water corals, high-resolution hydrodynamic modeling is employed. These frameworks help to identify key sources, sinks, and corridors of coral larvae (reproductively produced propagules; Guy and Metaxas, 2022; Metaxas et al., 2019). For corals on the shelf and slope off Newfoundland and Labrador, these modelling approaches show that the strong Labrador Current underpins much of the potential connectivity from north to south along the shelf edge and make larval transport into the High Seas possible (Le Corre et al., 2018). This is consistent with studies by Wang et al. (2020) and Kenchington et al. (2019) who highlight the importance of the Labrador Current and Deep Western Boundary Current on the dispersal of larvae on the eastern side of the Grand Banks even beyond 1000 m depth. In fact, these approaches have shown that the southern flanks of the Flemish Cap seem to experience faster currents at depth (1000 m) than near the surface (100 m) due to the influence of the Gulf Stream and North Atlantic Current (NAC); these systems meander to the northeast in a region characterized by strong surface and sub-surface eddy activity (Kenchington et al., 2019; Schubert et al., 2018). Connectivity studies were also carried out further south along the US and Canadian coasts. Wang et al. (2022, 2021) investigate the dispersal of larvae in the Gulf Stream and along the coast of Nova Scotia in particular. Their results yet again show the major impact of the fast-moving currents in the region, but also the importance of variability associated with eddies and topographic features, for connectivity patterns. Therefore, coral larvae dispersal to and from the *Titanic*, and thus the role the wreck plays in marine connectivity further afield, is likely a product of a complex interplay between various hydrographic features and ocean dynamics from the surface to the seafloor.

Biophysical hydrodynamic models that incorporate larval behavioral traits (e.g., timing of spawning, larval duration, vertical and horizontal swimming behaviors) provide idealized representations of potential larval dispersal pathways and thus, patterns of connectivity (Hilário et al., 2015). But for most deep-sea corals including those found on the *Titanic*, such life history information is entirely absent (Waller et al., 2023), which limits the applicability of a single experiment (Gary et al., 2020). Instead, multiple scenarios that experiment with different larval behaviors can help to establish levels of uncertainty but also a consensus view on the dispersal potential of corals from *Titanic*'s and its wider natural heritage legacy in terms of marine connectivity. Viewing

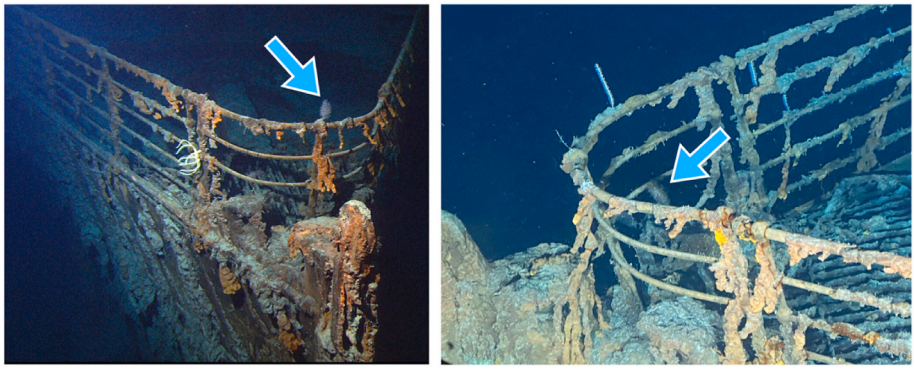

Fig. 1. Photos of RMS *Titanic* bow. Left: photo from 2004 (credit NOAA Ocean Exploration and Research) with *C.* cf. *agassizii* in the center of the top rail (blue arrow). Right: photo from 2021 (credit Ocean Gate Expeditions) showing *C.* cf. *agassizii* in a different position on the bow (blue arrow). Note that there are other attached octocorals, some of which may be *Chrysogorgia* spp. and/or *Lepidisis* spp.

dispersal models more as possible outcomes rather than true or actualized dispersal (Ross et al., 2020) can also help identify possible upstream sources of larvae arriving at the *Titanic* and whether slope to abyssal larval dispersal could be significant. It can also investigate the likelihood of the wreck site now acting as a stepping stone connecting to downstream populations. In doing so, these experiments can also inform future studies on the reproductive biology of *C. agassizii* by identifying which larval behavior traits, if any, impart variability in connectivity patterns.

For more realistic representations of dispersal, biophysical models need to include the full spatio-temporal range of the underlying ocean circulation. Of particular importance is the mesoscale circulation at scales of 10–100 km that covers oceanic fronts, eddies and detailed boundary current structures. In addition to their importance for mixing water across fronts, eddies are also an important part of the large-scale circulation and are present in vast areas of the world oceans (Chelton et al., 2007, 2011). In the North Atlantic, individual eddies transport water over large distances, contributing to the transport of heat and freshwater (Müller et al., 2019). Experiments on the upper-ocean dispersal have shown that advective patterns and transfer time scales can be quite sensitive to the grid resolution of the physical ocean model (Blanke et al., 2012; Bonhommeau et al., 2009). For the deeper ocean, grid resolution is important to correctly include topographic features like slopes, trenches, gaps or ridges. Seafloor bathymetry has a direct impact on the dispersal of benthic organisms by steering, or blocking, the flow and needs to be adequately represented (Breusing et al., 2016). As the underlying physical model, we use the high-resolution model VIKING20X that covers the Atlantic at 1/20° horizontal grid resolution. VIKING20X has been proven to realistically simulate various features of the Atlantic circulation from basin-scales down to the mesoscale (Biastoch et al., 2021; Rieck et al., 2019; Rühs et al., 2021) and is also often the basis for dispersal studies (e.g. Busch et al., 2021). Its predecessor VIKING20, restricted to the North Atlantic, has demonstrated its performance to simulate the deep circulation (Breusing et al., 2016; Schubert et al., 2018).

The *Titanic*'s location in ABNJ, protection under UNESCO and multilateral agreements, cultural significance, natural heritage and the wreck's location in a highly complex oceanographic region, make the wreck site of the RMS *Titanic* a unique case study to launch an interdisciplinary investigation into the role shipwrecks play in marine connectivity. The rapid deterioration of the *Titanic* (Bright et al., 2005), the vulnerability of natural deep-sea coral populations to climate change (Morato et al., 2020) and human activities that fragment or degrade coral habitats (Ragnarsson et al., 2017) make it important to understand whether the *Titanic* and other shipwrecks could confer resilience to networks of marine populations. Given the importance of understanding population connectivity as part of Atlantic basin scale ecosystem assessment (Roberts et al., 2022) and the increasing amount of anthropogenic material in the deep ocean, including underwater cultural heritage such as shipwrecks (Meyer-Kaiser and Mires, 2022), experiments with virtual larvae released from shipwrecks will help us understand the dispersal potential of species from the *Titanic* and the natural heritage legacy this and other wrecks could play in terms of marine connectivity. In the following, we aim to answer two main questions:

- Where does larvae spawned at the *Titanic* wreck disperse to and which circulation conditions and larval characteristics control it?
- Is the *Titanic* connected to known occurrences of cold-water corals along the Northwest Atlantic continental slope?

2. Methods

2.1. Model configuration: VIKING20X

This study is based on a hindcast simulation of the global, nested VIKING20X ocean - sea-ice model configuration (Biastoch et al., 2021). The ocean component is provided by the NEMO v3.6 model and the sea-ice component by the Louvain la Neuve Ice Model (LIM2; Fichefet and Maqueda, 1997; Vancoppenolle et al., 2009). VIKING20X consists of a 1/20° nest grid, embedded within a global 1/4° grid. At the *Titanic* position this corresponds to a horizontal grid spacing of approximately 4 km.

The nest covers the Atlantic Ocean from the southern tip of Africa to approximately 65°N. Both grids exchange information via a 2-way coupling utilizing the Adaptive Grid Refinement In Fortran (AGRIF) package (Debreu et al., 2008). The vertical grid consists of 46 z-levels with increasing spacing from 6 m at the surface to about 250 m at the deepest level (about 240 m at the *Titanic* depth). Partial steps are used for a better representation of bathymetric gradients (Barnier et al., 2006).

The momentum advection equation is discretized using the energy and enstrophy conserving (EEN; Arakawa and Hsu, 1990; Ducousso et al., 2017) scheme. Momentum diffusion is accomplished by application of a bi-Laplacian operator acting along geopotential surfaces with a viscosity of 15×10^{10} m^4s^{-1} (nest grid: 6×10^9 m^4s^{-1}). The tracer advection equation is discretized using the total variance dissipation scheme (TVD; Zalesak, 1979). Tracer diffusion is accomplished by a Laplacian operator along iso-neutral surfaces with an eddy diffusivity of 300 m^2s^{-1} (nest grid: 600 m^2s^{-1}).

On both grids free-slip lateral momentum boundary conditions are applied. Only on the nest grid, no-slip boundary conditions are applied around Cape Desolation to improve mesoscale activity to the west of Greenland (Rieck et al., 2019).

The model experiment used for this study is referred to as VIKING20X-JRA-SHORT (see Biastoch et al., 2021). This experiment is initialized in 1980 branching of from an experiment performed under the CORE2 (Griffies et al., 2009; Large and Yeager, 2009) surface forcing initialized in 1958 following a 30-year spin-up. VIKING20X-JRA-SHORT is then run until 2019 under the JRA55-do v1.4 (Tsujino et al., 2018) surface forcing. It uses a weak Sea Surface Salinity restoring with a timescale of 12.2 m yr^{-1} and no freshwater budget correction.

2.2. GLORYS12v1 – ocean reanalysis

The performance of VIKING20X is validated by comparison of the mean circulation, variability and trajectories itself to the GLORYS12v1 reanalysis (Copernicus Marine Service Information, 2023). GLORYS12 is based on the NEMO ocean model and uses a 1/12° global grid with 50 depth levels (Lellouche et al., 2021). GLORYS12 assimilates various observations, such as sea surface temperature derived from satellites and vertical profiles of temperature and salinity. GLORYS12 does not assimilate observations at the depth of the *Titanic* wreck site. A connection between variability in the upper and deep ocean still is still expected to result in different representations of the flow at depth in GLORYS12 and VIKING20X. Although GLORYS12 is run on an Arakawa C-grid, the publicly available data is provided on an A-grid. Horizontal current velocities from GLORYS12 are available from 1993 to 2023 and stored at daily resolution. Note that vertical velocities and horizontal velocities on the native C-grid, which would be needed for an accurate calculation of vertical velocities based on volume conservation, are not published.

2.3. Lagrangian experiments

To study the fate and potential source of *C. agassizii* larvae at the *Titanic*, we run a set of Lagrangian experiments, using the Parcels (version 2.2.1) Python package (Delandmeter and van Sebille, 2019).

Parcels solves the advection equation numerically. Here the fourth-order Runge-Kutta scheme, including vertical velocities is applied with a numerical timestep of 10 min. No diffusion parameterization scheme is used in the calculation of trajectories, a choice that is thoroughly discussed by Rühs et al. (2018). As input fields, the 5-day averaged output

of VIKING20X on the nest grid is used. Within parcels these fields are linearly interpolated to the current time step.

We release 10,000 particles on the first day of each month from 2009 to 2018, resulting in 120 release experiments (1.2 million particles in total). The aim of this release strategy is to capture the impact of flow variability on timescales from months to years. It was verified that the number of released particles is sufficient by evaluating different subsamples with reduced size. Metrics, such as the area that contains 95% of the particle occurrences, converge rapidly after 1000–2000 particles. All trajectories within the release experiment are integrated forward in time for 90 days.

The larval characteristics of *C. agassizii*, including larval longevity, are currently not known. Most octocoral larvae studied so far, including shallow tropical (Ben-David-Zaslow and Benayahu, 1998; Coelho and Lasker, 2016), temperate (Guizien et al., 2020), and deep-sea species (Rakka et al., 2021b; Sun et al., 2010) can survive without settling for 20–90 days and up to a year (Rakka, 2021a). Based on this information, we chose 90 days as our best estimate of larval longevity for *C. agassizii*. Although the chosen 90 days are considered realistic, deep-sea coral larvae can survive longer (e.g. Larsson et al., 2014), thus our results present a conservative estimate of the possible spreading.

All Lagrangian experiments analyzed here are described below and summarized in Table 1. Additional Lagrangian experiments used to validate the VIKING20X trajectories can be found in the supplementary data (Table S1).

2.3.1. Releases from the Titanic

We seed particles horizontally around the *Titanic*'s position (coordinates of the bow section) according a random normal distribution with a standard deviation of 0.025° in latitude and $0.025/\cos(\phi)$° in longitude direction, where ϕ is the center latitude of the release. This corresponds to a distance of 2.8 km in both cases. Experiments were focused on the bow section of the wreck site where most putative *C. agassizii* had been previously observed. Particles are initially placed 10 m above the actual depth at the *Titanic* site (at 3810 m) to simulate this position on the bow. If the seafloor in the model is shallower than this depth, we release particles 10 m above the grid-cell floor.

In a first experiment, referred to as EXP_{pas}, particles are advected purely passive in the ocean currents as simulated by the model (20 exemplary trajectories are shown in Fig. 2). We use the full 4-dimensional output of the model, including depth, which was found to be important for the dispersal in a nearby area (Wang et al., 2020). In a second experiment, referred to as EXP_{act}, particles can actively swim in the vertical direction, a behavior that has been reported for several deep-sea benthic species (Arellano, 2008; Beaulieu et al., 2015; Yahagi et al., 2017) including deep-sea corals (Larsson et al., 2014). Since there is currently no information on the larval traits of *C. agassizii*, in this experiment we use values for swimming speed and larval duration reported for larvae of *Viminella flagellum*, which is the only deep-sea octocoral with vertical swimming behavior of its larvae known so far (Rakka, 2021a). The selected swimming speed is close to the highest speeds that have been reported for other octocoral species (e.g., Martínez-Quintana et al., 2015; Rakka et al., 2021b), serving the purpose of this experiment to provide an upper limit for the potential impact of active behavior of the larvae on the dispersal. Based on very little information available, we assume a pelagic larval duration (PLD) of 6 days. Possible implications of a longer PLD are discussed later. Accordingly, larvae in EXP_{act} swim upward with a constant velocity of 1.5 mm/s for 6 days and then downward with the same constant velocity until they get closer than 10 m to the seafloor. After swimming terminates, particles passively drift until the end of the experiment.

Additional experiments are conducted using temporally averaged velocity fields to study the contribution of the mean flow and seasonal to interannual variability to the dispersal from the *Titanic* wreck. In these experiments particles are released only once and the velocity is steady for the entire length of the experiments (90 days). In EXP_{mean} the 10-year averaged velocity field between 2009 and 2018 is used. The purpose of this experiment is to study the contribution of the mean flow to the dispersal of larvae from the wreck site. In EXP_{yr}, particles are released in the annual mean velocity field for all years from 2009 to 2018, which results in 10 release experiments. EXP_{yr} provides information about the importance of interannual variability on the dispersal pathways. To study the impact of seasonal variability, we release particles in the climatological velocity field of all month (monthly climatology for years 2009–2018), which results in 12 releases. This experiment is referred to as EXP_{clim}.

In order to validate the models performance in simulating realistic Lagrangian trajectories, we compare the trajectories obtained from VIKING20X (EXP_{var} and EXP_{mn}) to similar experiments based on velocity fields from GLORYS12 (see supplementary data).

2.3.2. Releases from natural occurring populations to the Titanic

In addition, we run three experiments to study population connectivity between the abyssal setting of the *Titanic* and sites in the Northwest Atlantic. Records of *C. agassizii* were obtained from a subset of data compiled from multiple sources (Ramiro-Sánchez et al., 2020) and an additional location reported by (Baker et al., 2012). The general release strategy described in section 2.3.1 for EXP_{pas} did not change, but only 12 release months are used (January–December 2009). This is sufficient, as the two previous experiments suggest interannual variability to be

Table 1
Overview of experiments. The *Titanic* is located at 41.73°N 49.95°W (3820 m), P1 is located at 46.07°N 47.61°W (400 m), P-B12 is located at 44.8°N 54.8°W (2000 m).

Experiment	Release (position)	Velocity field	Release (time)	Runtime in days	Active motion	Motivation
EXP_{pas}	*Titanic*	VIKING20X: 5-day means	monthly (2009–2018)	90	–	Dispersal from the *Titanic*
EXP_{act}	*Titanic*	VIKING20X: 5-day means	monthly (2009–2018)	90	6 days upward swimming then sinking (1.5 mm/s)	Impact of swimming on dispersal from the *Titanic*
$EXP_{P1\text{-}P2}$	P1	VIKING20X: 5-day means	monthly (2009)	180	–	Timescale of spreading along the upper slope (P1 to P2)
EXP_{P1_T}	P1	VIKING20X: 5-day means	monthly (2009)	90	30 days passive then sinking (1.5 mm/s)	Larval characteristics needed for direct connectivity between P1 and the *Titanic*
EXP_{T_P2}	*Titanic*	VIKING20X: 5-day means	monthly (2009)	180	–	Assess sensitivity of dispersal from the *Titanic* on larval longevity
EXP_{B12}	P-B12	VIKING20X: 5-day means	monthly (2009)	180	–	Connectivity of the Titanic to a natural occurrence in close proximity
EXP_{mean}	*Titanic*	VIKING20X: 10-year mean (2009–2018)	once	90	–	Contribution of the mean flow to the dispersal from the *Titanic*
EXP_{yr}	*Titanic*	VIKING20X: annual averages	once per year (2009–2018)	90	–	Contribution of interannual variability to the dispersal from the *Titanic*
EXP_{clim}	Titanic	VIKING20X: monthly climatology	once per month	90	–	Contribution of seasonal variability to the dispersal from the *Titanic*

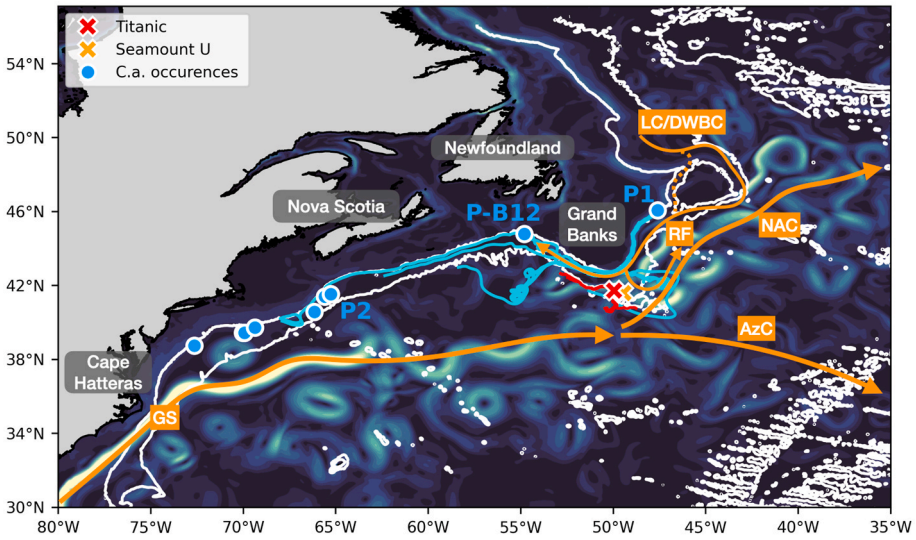

Fig. 2. Surface velocity snapshot in VIKING20X (model day 15-10-2009). The red cross marks the *Titanic* position and blue dots indicate known positions of *C. agassizii*. The orange cross marks the Seamount U. The 1000 and 3500 m isobaths are shown in white. Exemplary trajectories from EXP_{pas} (red; length: 30 days) and $EXP_{P1\text{-}P2}$ (blue; length: 180 days). Major currents are indicated by arrows (GS: Gulf Stream, NAC: North Atlantic Current, AzC: Azores Current, LC: Labrador Current, DWBC: Deep Western Boundary Current, RF: Labrador Current Retroflection).

negligible compared to monthly variability.

A first experiment ($EXP_{P1\text{-}P2}$) is run to study the timescale of spreading from a known population of *C. agassizii* east of the Grand Banks (labeled as P1 in Fig. 2), to a population on the Nova Scotian Slope (labeled as P2 in Fig. 2). The purpose of this experiment is to answer questions on dispersal pathways along the upper continental slope and to identify possible locations, where larval particles could leave the boundary towards the *Titanic* position. Particles are passively advected without any active behavior for 180 days. Especially because we are mainly interested in the advective timescale set by the ocean currents and there is little information about the larval biology, a passive experiment is the most appropriate choice and does not require any assumptions. Again, a similar experiment is conducted in GLORYS12 to validate the trajectories (see supplementary data).

Motivated by the results of this experiment, a second experiment ($EXP_{P1\text{-}T}$) is conducted to study whether larvae from this known occurrence (P1) on the upper slope could reach the deeper lying *Titanic* wreck. Therefore, we set up an experiment where particles spread purely passive for 30 days and then sink with a constant velocity of 1.5 mm/s until they get closer than 100 m to the seafloor. Afterward, larvae can passively drift until an age of 90 days. We use the same speed as for EXP_{act}, as a fast downward motion increases the likelihood of connectivity, but at the same time the downward velocity should be achievable by the larvae. The onset of downward motion after 30 days is based on various short experiments showing that an onset of downward motion after 30 days makes a connection to the *Titanic* most likely. This experiment is therefore meant to provide information on the larval behavior that is needed for a direct connectivity to exist, rather than an estimate of the true dispersal.

In a third experiment ($EXP_{T\text{-}P2}$) we assess, whether our results on connectivity from the *Titanic* to the downstream population (P2) of *C. agassizii* are changed by doubling the assumed larval longevity. Therefore, we repeat EXP_{PAS}, but with a runtime extended to 180 days.

A last experiment is run to study whether the observed occurrence of *C. agassizii* reported in Baker et al. (2012) within the Canadian EEZ at 2000 m depth (P-B12; Fig. 2) could be a possible source population of corals at the *Titanic*, or might act as a stepping stone connecting the *Titanic* to P2 ($EXP_{P\text{-}B12}$).

3. Results

3.1. Oceanographic setting and model validation

Before we analyze and interpret the results of the Lagrangian experiments, we describe the general circulation in the region of interest and verify that it is reasonably represented in VIKING20X by comparing it to observational data and ocean reanalysis. The *Titanic* wreck site is located in waters approximately 3800 m deep, but direct (especially long term) measurements at this site are very sparse, or not available, at these depths. Therefore, we focus on the representation of major currents and mesoscale variability at the surface and mid-depth, that will be shown to strongly impact our results.

3.1.1. Gulf Stream and North Atlantic Current

The near surface circulation along the United States' east coast is dominated by the northward flowing Gulf Stream (GS) that separates from the coast near Cape Hatteras (35°N) and continues north-eastward. At the Tail of the Grand Banks the GS splits into the north-eastward North Atlantic Current (NAC) and an eastward branch called Azores Current (Daniault et al., 2016; Frazão et al., 2022). This general description also holds for the model as evident in Fig. 2.

The mid-depth circulation, as derived from ARGO floats at a depth of approximately 1000 m (ANDRO dataset; Ollitrault et al., 2022), shows the GS centered around 39°N (Fig. 3a). The modelled and observed mean velocity maxima are similar in magnitude at most longitudes, but cover a smaller latitude range and appear about 1.5° further south in the model west of approximately 55°W (Fig. 3b). However, as the Gulf Stream splits into the Azores Current and NAC at approximately 51°W the maximum EKE in the model and the ANDRO dataset are found at similar latitudes. This is further supported by the position of the 15 °C isotherm at 200 m depth, indicative of the GS path, which matches observations very well at the Tail of the Grand Banks (Fig. 3b; Seidov et al., 2019). The NAC position and pathway is in good agreement with observations. Note that the ANDRO dataset is based on 3° × 3° binned float displacements and can only provide a smoothed representation of the flow field.

The GS/NAC flow is characterized by strong meanders and mesoscale eddies known as Gulf Stream Rings (Ducet and Le Traon, 2001; Schubert et al., 2018). Eddies north of the main GS axis are predominantly anticyclonic, carry a positive temperature anomaly and are also known as

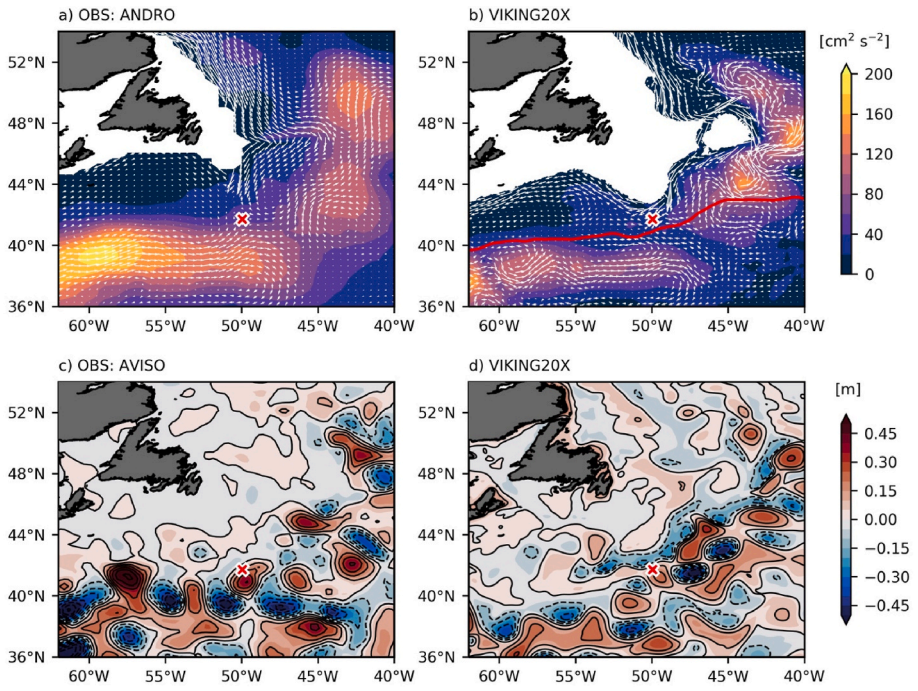

Fig. 3. Eddy Kinetic Energy and mean currents at approximately 1000 m (950–1150 m) depth based on the ARGO derived ANDRO dataset (a) and VIKING20X (b; 1980–2018). Velocity vectors scale with the speed up to 15 cm/s. Snapshots (5-day mean) of the spatially high-pass filtered SSH anomaly in AVISO (c, 05-08-2010) and VIKING20X (d,15-10-2009). The *Titanic* is marked with a red cross. The red contour in b) shows the mean position of the 15 °C isotherm at 200 m depth (1980–2018) in VIKING20X.

Warm Core Rings (Brown et al., 1986; Saunders, 1971). Sea Surface Height (SSH) anomaly fields derived from satellite altimetry (AVSIO; Taburet and Pujol, 2022) show that surface eddies are found further south in observations west of the *Titanic* position. However, at the *Titanic* position and along the NAC pathway the position of eddies in the VIKING20X model and the AVISO dataset are found at similar locations (Fig. 3c and d). In both snapshots eddies are seen above the wreck site. Thus, at the Tail of the Grand Banks the position of eddies and meanders associated with the GS/NAC are well captured by the model. The SSH anomaly associated with eddies appears to be underestimated west of the *Titanic* position, but is again more similar once the GS turns northward south of the wreck site (Fig. 3c and d).

In addition to Gulf Stream Rings that are clearly visible at the surface, meanders of the GS/NAC can drive deep cyclogenesis, and these deep mesoscale features can cause benthic storms, i.e., strong velocity anomalies near the bottom, as evidenced by both ocean-based observations and the VIKING20X model (Schubert et al., 2018; Shay et al., 1995). It is therefore important to also validate the variability at mid-depth. Eddy Kinetic Energy (EKE), the kinetic energy contained in deviations from the time mean circulation (and in parts associated with mesoscale variability), at mid-depth is underestimated west of 55°W compared to the ANDRO dataset and the GLORYS12 reanalysis (see also Fig. S1). This is consistent with the upper description of mesoscale variability at the surface (Fig. 3c and d). East of 55°W the magnitude of EKE is in better agreement with the ANDRO dataset. At the *Titanic* position itself, EKE is slightly underestimated. Still, surface and mid-depth eddies associated with the GS/NAC current system are present in the model above the wreck site and EKE values at mid-depth are clearly higher than in the ocean interior (Fig. 3a and b). The depth structure of EKE in the model shows that high EKE values associated with the GS and NAC extend to the sea-floor (Fig. S1). A meridional section at 55°W, as well as a zonal section at 48°N show EKE values between 50 and 100 cm^2/s^2 to extend beyond 4000 m depth. At 48°N, the structure, as well as the magnitude, of EKE are in good agreement with observations, other models and the GLORYS12 reanalysis (De Verdière et al., 1989; Smith et al., 2000; Figs. S1a and c). The magnitude of EKE is underestimated along the GS at 55°W throughout the whole water column compared to GLORYS12 (Figs. S1b and d; see also Richardson, 1983). Vertical profiles of the mean and eddy kinetic energy in the region around the Grand Banks in VIKING20X are consistent with other high-resolution models and GLORYS12 (Zhai et al., 2015; Fig. S1e). Overall, these results highlight the ability of the VIKING20X model to reproduce the vertical structure of the circulation's variability in the region of interest for this study. The slightly different representation of the GS at 55°W has minor impacts on the dispersal of larvae along the continental slope, as shown in section 3.2.

3.1.2. *Labrador Current and Deep Western Boundary Current*

From the Labrador Sea, the Labrador Current transports water southward along the slope in the top 600 m. The Deep Western Boundary Current (DWBC) is responsible for a southward transport of more dense water below the LC (New et al., 2021, Fig. 2).

Since it is especially important for our study of connectivity, Fig. 4a shows a velocity section on the eastern side of the Grand Banks (east of Flemish Cap) at 47°N. The long term mean velocity structure in the model agrees well with the mean structure derived from lowered acoustic doppler current profilers (LADCP). The LADCP measurements were conducted during 9 ship sections between 2003 and 2017. The dataset was published by Mertens et al. (2019) and is described in Rhein et al. (2019). The main core of the DWBC is found above the continental slope with a maximum speed of 30 cm/s at approximately 2000 m depth in both, the VIKING20X model and LADCP observations. A secondary, bottom intensified, core can be seen above the continental rise. Further east, the mean velocity is northward associated with the NAC that extends to the seafloor. Also the southward flow associated with the Newfoundland Basin Recirculation Gyre (Bower et al., 2009; Mertens et al., 2014) is visible in the model. The close match between the model and observations highlights that VIKING20X is capable to simulate details of the mean flow at depth. This comparison shows that the performance east of Flemish Cap is comparable to its predecessor VIKING20

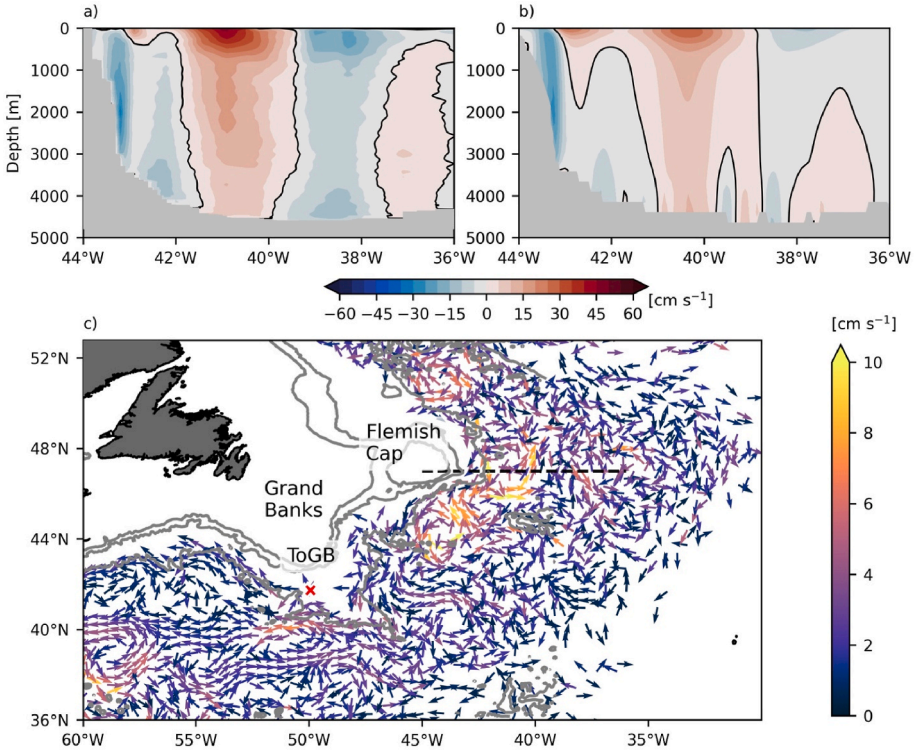

Fig. 4. Mean velocity section at 47°N derived from ship-based measurements (Mertens et al., 2019; a) and from the VIKING20X model (1980–2018; b) The position of the section is indicated by a dashed black line in panel (c) along with the mean velocity (1980–2018) at 3650 m depth. The *Titanic* is marked with a red cross. The grey line indicates the 500, 2000 and 4000 m depth contours. ToGB – Tail of the Grand Banks.

that was documented by Mertens et al. (2014).

South of 47°N the LC and DWBC continuously follow the continental slope and turn west around the Tail of the Grand Banks (Schott et al., 2004, Fig. 2). The main core of the DWBC at mid-depth is located to the north of the *Titanic* (Fig. 3a and b). At the Tail of the Grand Banks a considerable amount of water recirculates northward in the Labrador Current Retroflection (e.g. Fratantoni and McCartney, 2010). In the model as well as in observations the retroflection occurs just east of the *Titanic* position. The retroflection is strongly affected by the interaction of GS/NAC meanders and eddies with the LC (Gonçalves Neto et al., 2023; Jutras et al., 2023). Therefore, the presence of the LC retroflection in model again indicates that meanders and eddies originating from the GS and NAC can reach the *Titanic* position.

The interaction of these eddies and meanders with the southward currents along the boundary can generate strong mesoscale activity itself. For example, Brickman et al. (2018) find westward moving eddies that are generated by an interaction of the GS with the LC. The presence of strong mesoscale activity at the Tail of the Grand Banks is further supported by the several in-situ and virtual float release experiments. Bower et al. (2013, 2009), Gonçalves Neto et al. (2023) and Jutras et al. (2023) all find floats advected southward in the LC/DWBC to leave the western boundary at the Tail of the Grand Banks in strong meanders or eddies. Furthermore, submesoscale eddies of subpolar origin, known as submesoscale coherent vortices, were shown to form south of the Grand Banks. They have a subsurface maximum and propagate west- or southward (Bower et al., 2013). The Tail of the Grand Banks is one of the most complex regions of the Atlantic with several energetic currents interacting with each other and with mesoscale and submesoscale circulation features that can emerge from various sources. VIKING20X is capable to simulate these complex interactions and the resulting strong mesoscale activity.

3.1.3. *Mean flow at the Titanic depth*

The *Titanic* itself, at a depth of 3800 m, is shielded from a westward flow by the Newfoundland Ridge extending south from the Tail of the Grand Banks. The flow follows the 4000 m depth contour in southwestward direction around the Tail of Grand Banks in agreement with other model results (Han et al., 2008). The water flows around the Newfoundland Ridge and then diverts into a pathway that continuous westward and a secondary pathway that turns to the northwest towards the *Titanic*. The latter forms a weak current along the bathymetry (Fig. 4c).

The flow away from the boundary is predominantly east and northward, but follows strongly meandering pathways with several recirculations, especially north of 42°N. This is probably a result of strong variability caused by the interaction between the DWBC and NAC and high eddy activity (Bower et al., 2011; Schott et al., 2004).

Overall, VIKING20X is able to simulate narrow currents along the shelf break with realistic velocities throughout the water column and a highly variable and deep reaching GS/NAC (see also Biastoch et al., 2021). In particular, the model is able to realistically simulate the interaction of the GS/NAC with the LC/DWBC at the Tail of the Grand Banks (above the *Titanic* wreck site). The deep flow and its variability upstream of the wreck site are in agreement with observations. VIKING20X simulates a realistic depth structure of EKE in the region around the Grand Banks, but underestimates the energy contained in mesoscale variability near the surface and in mid-depth above the *Titanic*, compared to observational data and other models. The depth structure of EKE within the GS and NAC are in agreement with other high-resolution models and observations north and south of the wreck site. This provides confidence that the model is able to simulate realistic flow variability also at depth. Although the Gulf Stream is located too far south west of 55°W, this has no major impacts on the variability at the wreck site, where the position of the GS and associated meanders and eddies is in good agreement with observations. The magnitude of mid-depth EKE along the continental slope, east of the Grand Banks (Fig. S1) and at the position of the *Titanic*, is similar in VIKING20X and GLORYS12, despite a different position of the GS axis at 55°W. This

suggests that a most of the variability at the wreck site is associated with the LC/DWBC and its retroflection, which is well represented in VIKING20X. It is therefore concluded that the circulation features that are deemed important for this study are reasonably well-represented. Further, VIKING20X, as well as its predecessor VIKING20, have demonstrated their ability to simulate deep flow variability in several studies (Biastoch et al., 2021; Handmann et al., 2018; Schubert et al., 2018; Schulzki et al., 2021). Therefore, the VIKING20X model is well suited to study the dispersal of larvae from and to the *Titanic*, but imperfections that are present in all models need to be kept in mind when interpreting the results. Because there are no long-term measurements available at the wreck site, or in close proximity, it is not possible to verify the models' ability to realistically simulate the circulation at the *Titanic* itself.

3.2. Larval dispersal from the RMS Titanic

When released at the *Titanic*, passive Lagrangian particles in EXP_{pas} follow two main pathways within the first 90 days after their release (Fig. 5a). One pathway follows the 3500 m isobath to the west. This pathway is diverted into a northern and a southern branch by a shallow (water depth 2500 m) seamount. The second pathway is directed south and bounded approximately by the 3500 and 4000 m isobaths. A comparison with EXP_{mean} reveals that the contribution of the mean flow is strongly limited. If the steady 10-year mean velocity field is used to advect particles, the dispersal follows the bathymetric contours, as expected for geostrophic flow (note that variations in depth are much more important here than variations in the Coriolis parameter). Additionally, the distance reached within 90 days from the wreck site is much smaller and the southward pathway is not existent, if temporal variability of the circulation is not considered (Fig. 5d).

To further investigate the mechanism that control the dispersal, Lagrangian experiments were conducted using the annual mean velocity fields between 2009 and 2018 (Fig. 5e). It is apparent that considering interannual variability of the circulation is not sufficient to explain the full dispersal pattern seen in EXP_{pas}. A similar conclusion can be drawn from EXP_{clim} for seasonal variability of the circulation. In EXP_{yr} and EXP_{clim} particles are still strongly confined to the depth contours and reach only limited distance from the wreck site (Fig. 5e and f). An insignificant number of particles can take a southward pathway, but only reach about 100 km from the wreck site.

This is further supported by calculating the probability distributions from EXP_{pas} for each season (based on the month of release) individually. As an example, Fig. 5c shows the distribution of all particles released in summer. The distributions for all seasons are shown in Fig. S2. They reveal that the pathways itself do not change with seasons, but are very similar to the distribution derived from all particles released in the experiment. The 95% contour extends similarly far west and south from the *Titanic* position in all seasons. This again demonstrates that subseasonal variability has a much larger impact on the dispersal pattern.

The limited distance from the wreck reached in the EXP_{mean}, EXP_{yr} and EXP_{clim} experiments and the mostly absent southward pathway, show that the subseasonal variability of the flow has a dominant impact on the dispersal pattern. It allows larvae to cross bottom contours, leading to much more diffusive pattern. Temporal variability on subseasonal timescales allows a significant number of larvae to follow a southward pathway and increases the distance reached from the *Titanic*

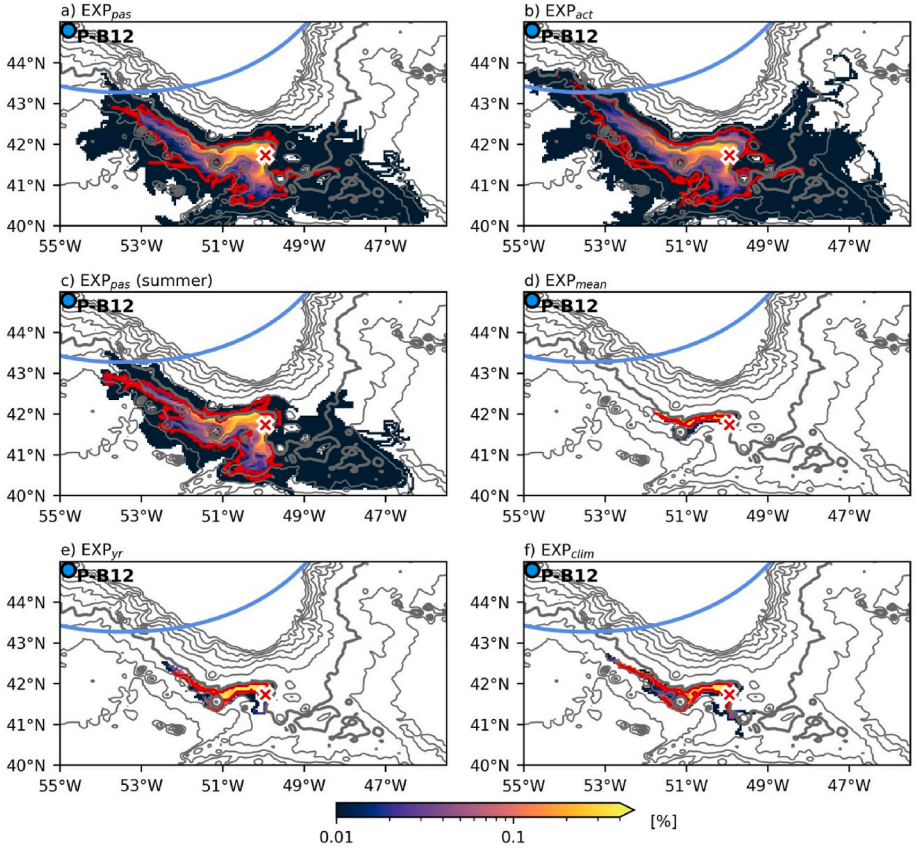

Fig. 5. Probability of particles to be found within 0.05° × 0.05° bins within 90 days after release. Particles are only counted once per bin. a) All particles released in EXP_{pas} and b) all particles released in EXP_{act}. c) Only particles in EXP_{pas} that are released in summer. d) Particles released in EXP_{mean} in a 10-year (2009–2018) averaged velocity field. e) Particles released in EXP_{yr} in the 10 annually averaged velocity fields of years 2009–2018. f) Particles released in EXP_{clim} in 12 climatological mean monthly velocity fields (climatology based on years 2009–2018).

in the westward (mean flow) direction. In particular, westward or southward spreading is not determined by seasonal or interannual, but shorter, variations of the deep circulation. These results are supported by passive Lagrangian experiments conducted in the GLORYS12 ocean reanalysis (Fig. S3).

A comparison of Fig. 5a and b shows that including active vertical movement does not lead to strong differences in the dispersal of larvae. The qualitative description of the pathways for EXP_{pas} above is still valid for EXP_{act}. The 95% contour line extends further west, indicating that the distance larvae can reach from the *Titanic* slightly increases. In our experiments, larval particles can swim upward with 1.5 mm/s for 6 days (777 m in total) and thus reach a depth of about 3000 m. As will be shown later, the circulation features that govern the dispersal do not have a strong velocity shear in this depth range. Therefore, the dispersal remains quite similar in the two experiments, and the swimming velocity that was defined in this experiment does not greatly impact the spreading in relation to the variability of ocean currents.

At the same time, the minor change in distance reached from the *Titanic* in EXP_{act} does allow for a considerable number of larval particles (indicated by the 95% contour) to reach the Canadian Exclusive Economic Zone (EEZ; EEZ boundaries were obtained from the Flanders Marine Institute (2019) Maritime Boundaries Geodatabase). In the passive dispersal scenario (EXP_{pas}), few particles can reach the EEZ, even under particularly strong circulation conditions (Fig. 5a). Although larval particles get close to the natural occurrence of *C. agassizii* (P-B12; Fig. 5) reported in Baker et al. (2012), their spreading is confined to regions offshore the 3500 m isobath, while P-B12 is located at 2000 m depth. Thus, direct connectivity is only possible with longer larval longevity than 90 days and higher vertical swimming capabilities than expected.

A direct dispersal from the *Titanic* to the aforementioned populations of *C. agassizii* P1 and P2 (Fig. 2) does not seem to be possible without additional stepping stones. There is no pathway to the north and larvae transported westward along the continental slope does not reach further than 55°W in any of the experiments. However, we do recognize that there are likely to be as yet undocumented habitats in the region that could be the stepping stones, which is further discussed in section 4.

3.3. Circulation conditions controlling the spreading

As shown in the last section, there are two main pathways of particles released at the *Titanic*. The Lagrangian experiments showed that subseasonal variability of the flow is much more important for the spreading than the mean flow and interannual or seasonal variations. We now study which physical mechanisms are associated with subseasonal variability that causes particles to spread either to the west or to the south. Therefore, we combine our Lagrangian experiments with a Eulerian analysis of the velocity field.

3.3.1. Velocity composites

We group all months by the dominant spreading direction in EXP_{pas} and calculate the composite velocity field of the respective months. For each release, we calculate the center of mass of all particles after 30 days. We chose to consider the position after 30 days, as we are interested in the processes that determine the initial dispersal from the wreck after release. These positions are shown in Fig. 6a. Subsequently, these positions are compared to the *Titanic* position. We group the release months according to the following equations:

$$\text{WEST: } lon_p(t_{rel}) < (lon_T - x_{thr})$$

$$\text{SOUTH: } lat_p(t_{rel}) < (lat_T - y_{thr})$$

$lon_p(t_{rel})$ and $lat_p(t_{rel})$ denote the coordinates of the center of mass of all particles released at time t_{rel} 30 days after the release. lon_T and lat_T are the *Titanic* wreck's (bow section) coordinates. x_{thr} and y_{thr} are 80% percentiles of lon_p and lat_p for all release months. As a result, the WEST group contains all release months, where particles spread anomalously far towards the west (24 release months; marked blue in Fig. 6a). The SOUTH group contains all months where particles spread anomalously far south (21 release months; marked purple in Fig. 6a).

Fig. 6b shows the mean circulation around the *Titanic*. The wreck is located in an embayment about 80 km in diameter, bounded by the Grand Banks and the Newfoundland Ridge, shielding it from a large-scale westward flow. Instead, it is characterized by a slow (<3.5 cm/s) cyclonic circulation along the bathymetry. The mean velocity is directed northward directly at the *Titanic* and turns westward further north. The

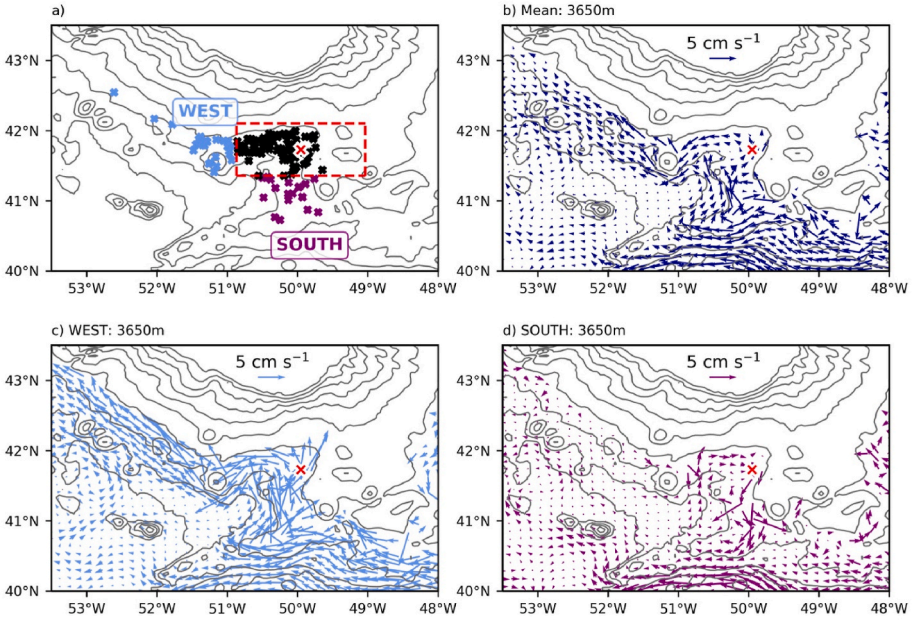

Fig. 6. a) Centre of mass of all particles released in a particular month in EXP_{pas}, classified based on anomalously strong westward (WEST; blue), or southward (SOUTH; purple) spreading. The red cross marks the *Titanic* position and the boundaries used for classification are indicated with dashed red lines. b) Mean (2009–2018) velocity at 3650 m depth. Composite velocity for subsets WEST (c) and SOUTH (d) at 3650 m depth. In all subpanels grey contours show the water depth with an interval of 500 m.

flow then continuously follows the bathymetry to the west.

During months of anomalous westward spreading the cyclonic circulation within the embayment is strongly enhanced (Fig. 6c). The composite velocity can exceed 10 cm/s. In contrast, the circulation reverses to anticyclonic flow during phases of strong southward spreading along the 3700 m isobath.

The composite of all months when spreading is neither anomalously west- nor southward, is nearly indistinguishable from the mean field (not shown). This is reasonable, since this group represents spreading under typical conditions. During normal conditions the particles tend to spread north-westward, but do not reach great distances from the *Titanic* (Figs. 6a and 5d).

In the following, we investigate the mechanisms causing the cyclonic circulation at depth to speed up, or to reverse. Therefore, we analyze composites of months with strong westward and southward spreading at shallower depth levels.

The composite of all months with strong westward spreading shows the presence of intense anticyclonic eddies located to the southeast of the *Titanic* at a depth of 1,000m (Fig. 7a). The western side of the eddies with north-eastward velocities is located directly above the wreck.

Also, strong southward spreading is associated with anticyclonic eddies at mid-depths (Fig. 7b). However, the eddies are located to the southwest of the *Titanic* and therefore velocities above this position are directed south-eastward.

As described before, these eddies can be of different origin. Mooring observations (Richardson et al., 1979) suggest that Gulf Stream Rings possibly extend to the seafloor, affecting the dispersal of larvae released in abyssal ecosystems. However, based on the near-surface composites (Fig. 7c and d), the circulation features affecting the dispersal must not have a clear surface signature. The near-surface circulation above the *Titanic* position is dominated by strong eastward velocities without a closed anticyclonic flow being visible in both cases. This suggests that in addition to Gulf Stream Rings, benthic storms driven by deep cyclogenesis and subsurface eddies of subpolar origin impact the spreading of larvae.

3.3.2. Characteristics of exemplary eddies

Composite means may not always represent true circulation, especially during extreme events. Therefore, we also provide the monthly mean velocity for the two release months with the strongest spreading in southward/westward direction. It is clearly visible in Fig. 8a and b that both events are associated with a strong mesoscale eddy at mid-depths, and both eddies are anticyclonic. For westward spreading, the center of the eddy is to the southeast of the *Titanic*, while it is to the southwest for southward spreading and therefore closely resembles the composite maps in Fig. 7.

A section through both eddies shows that their depth structure differs in the upper water column. While for the eddy in October 2009 (Fig. 8c) the strongest anomalies are found at the surface, the eddy in July 2011 is characterized by a subsurface maximum at 600 m depth (Fig. 8d). Accordingly, only the first eddy shows a pronounced surface signature. The second eddy is associated with a very weak anticyclonic circulation close to the surface only and no clear SSH anomaly (not shown). This suggests, in agreement with the composites, that not all eddies occurring south of the Grand Banks are Gulf Stream Rings with a detectable signature at the surface.

Despite these differences, both eddies are associated with deep velocity anomalies extending to the seafloor. Therefore, eddies can alter the deep flow (below the main eddy core) and affect the spreading of larvae from the *Titanic*. The first eddy does increase the northward flow into the embayment. At the longitude of the *Titanic* (dashed grey line in Fig. 8c) the velocity anomaly is positive and thus associated with stronger than average northward flow along the eastern side of the embayment. This anomalously strong northward flow into the embayment must turn westward as it approaches the northern boundary of the embayment at 3650 m depth. Therefore, the westward flow exiting the embayment is enhanced and particles from the *Titanic* can spread further to the west than under normal conditions. The second eddy is associated with an eastward velocity anomaly below 3000 m. At the latitude of the *Titanic* (dashed grey line in Fig. 8d) the eddy pushes water eastward into the embayment. An eastward flow along the northern boundary of the embayment must turn southward as it approaches the shallow bathymetry in the east. This southward flow is then responsible for

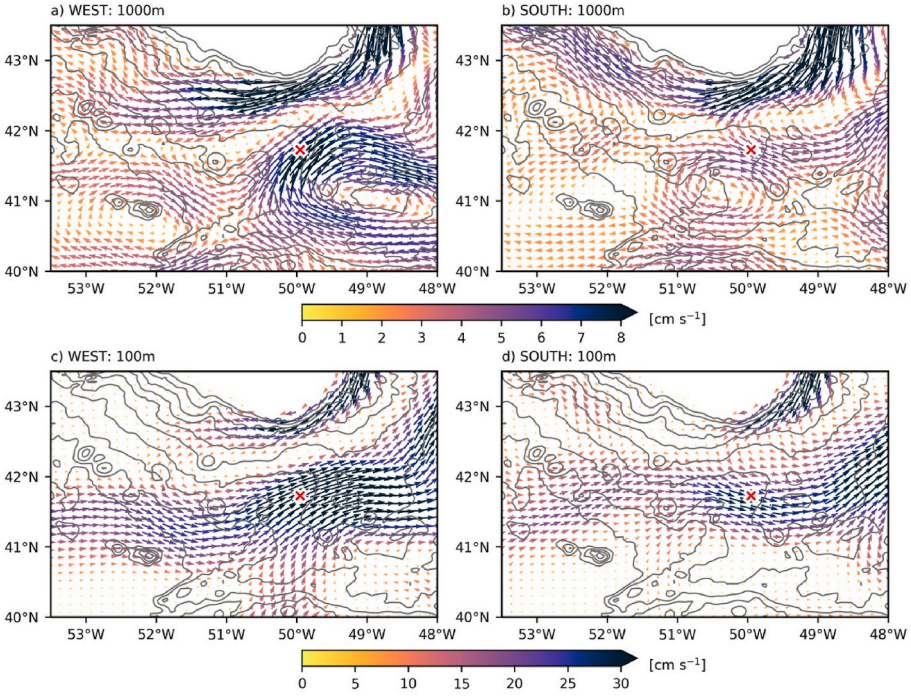

Fig. 7. Composite mean velocity at 1000 m depth based on all release month with strong westward (a) and southward (b) spreading. c), d) as a), b) but for 100 m depth. The *Titanic* is marked with a red cross. In all subpanels grey contours show the water depth with an interval of 500 m.

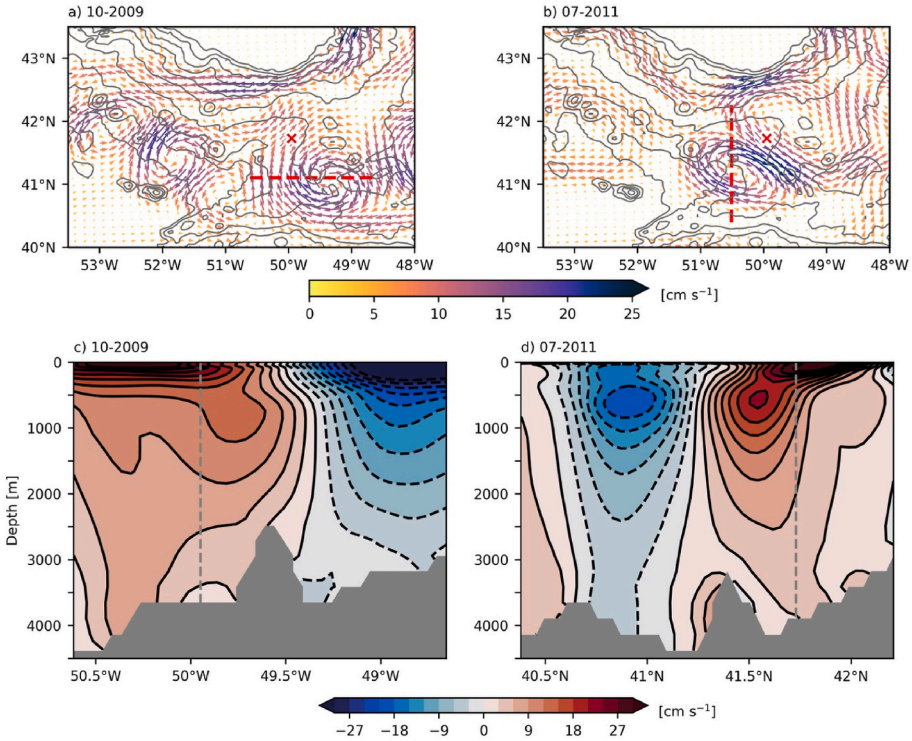

Fig. 8. Monthly mean velocity at 1000 m depth in the months of strongest westward spreading (10–2009; a) and strongest southward spreading (07–2011; b). The *Titanic* is marked with a red cross. Grey contours show the water depth with an interval of 500 m. c) Meridional velocity anomaly (10–2009) along the section shown in a). d) Zonal velocity anomaly (07–2011) along the section shown in b). The vertical grey lines indicate the latitude/longitude of the *Titanic*.

carrying larvae away from the *Titanic* towards the south.

The rather small vertical gradients in the velocity anomaly below 2500 m can also explain why active vertical movement does not strongly affect the spreading. Active swimming to shallower depths (in a realistic range) does not cause the particles to enter a different flow regime and thus does not greatly alter their pathways. In EXP_{act} particles reach a depth of about 3000 m. This is still well below the eddy core of both exemplary eddies. Note that also the mean flow does not show significant vertical gradients in the depth range covered by the larvae.

The circulation in individual months with anomalously strong spreading not always exactly resembles the corresponding composite mean, or the two exemplary snapshots shown here. Still, in most cases the presence of mesoscale structures is visible in the vicinity of the *Titanic*, causing the flow to have a strong northward (for westward spreading), or south-eastward (for southward spreading) component at mid-depth.

Mesoscale features therefore play a major role in VIKING20X, determining the direction and strength of the modelled spreading of larvae. However, particles are not entrained into and carried by the eddy itself. Instead, the abyssal circulation, strongly guided by the bathymetry, responds to the overlying eddy and causes the flow to be stronger than average in a westward direction, or to reverse. We find that all types of mesoscale features, deep cyclones generated below GS/NAC meanders, Gulf Stream Rings, and eddies of subpolar origin, may impact larval spreading. Meanders of the GS and Warm Core Rings north of the GS axis are anticyclonic (e.g., Brown et al., 1986). Also eddies of subpolar origin at the Tail of the Grand Banks are predominantly anticyclonic (Bower et al., 2013). This could explain the apparent dominance of anticyclonic eddies on larval trajectories. A dominant impact of eddies from subpolar origin is further supported by the similarity of the dispersal from the wreck in VIKING20X and GLORYS12 (Fig. 5 and S3). While differences exist in the position and variability of the Gulf Stream, variability associated with the LC retroflection is more similar in the two models.

3.4. Ecosystem connectivity along the Northwest Atlantic continental slope

After studying the fate of larvae spawned at the *Titanic* wreck the question arises, whether the *Titanic* is connected to other known populations of *C. agassizii*. Known occurrences of *C. agassizii* at the present time are marked in Fig. 9 (extracted from a subset of data compiled by Ramiro-Sánchez et al., 2020 and a position reported in Baker et al., 2012). As already mentioned, larvae cannot reach these locations directly assuming a maximum larval longevity of 90 days. Nevertheless, the more northerly occurrences and the occurrence at 'P-B12′ in close proximity to the wreck site could be sources for the *Titanic* population. The downstream ecosystems off Nova Scotia may be reached with a reasonable number of stepping stones. Possibly the *Titanic* could be a stepping stone itself connecting these populations to the slopes and seamounts of the Northwest Atlantic and into the Canadian EEZ.

3.4.1. Connectivity between naturally occurring populations

To study whether such a connectivity is possible, we release particles at the position labeled as 'P1′ in Fig. 9 ($EXP_{P1\text{-}P2}$). Population 1 is located north of the *Titanic*, at a depth of approximately 400 m. This location is directly influenced by the strong mean flow of the LC and DWBC along the continental slope.

A significant number of released particles continuously follow the bathymetry to the south (Fig. 9a) and reach P-B12 within 90 days. Population 2 ('P2′) is located further downstream the DWBC and connectivity to P1 is mostly determined by the larval longevity. In close proximity to P2 and in the downstream DWBC direction there are several more known populations. A connection to P2 would therefore also connect P1 to all of these populations. In VIKING20X, the fastest virtual particles reach P2 within 120 days (Fig. 9a). A similar result is obtained from the GLORYS12 ocean reanalysis (Fig. S4). Thus, only one additional population along the pathway would be required, if a maximum larval longevity of 90 days is assumed. P-B12 could be such a

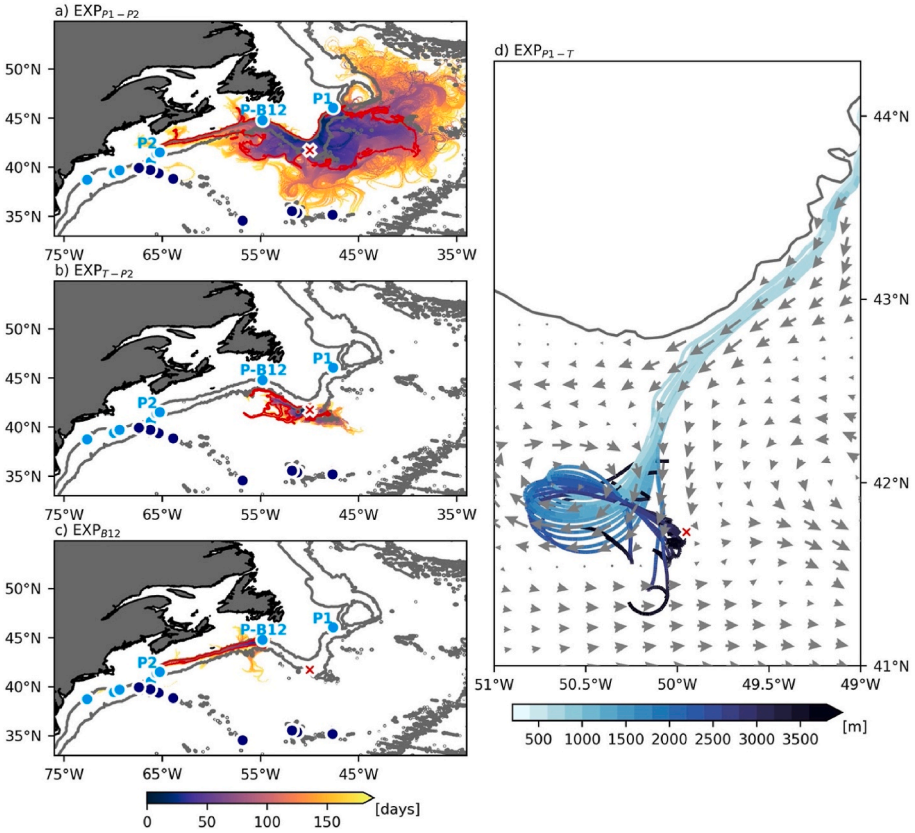

Fig. 9. Minimum age of particles when first arriving in 0.05° × 0.05° bins in $EXP_{P1\text{-}P2}$ (a). The red contour shows the 95% contour based on a corresponding probability map. Light blue dots show known populations of *Chrysogorgia agassizii* and dark blue contours known populations of other *Chrysogorgia* species. Grey contours indicate a water depth of 1000 and 3500 m. Same for $EXP_{T\text{-}P2}$ (b) and EXP_{B12} (c). Selected trajectories (length: 55 days) from $EXP_{P1\text{-}T}$ colored with their depth and 500 m velocity snapshot (06-08-2009; d). The grey line indicates the 500 m isobath. The *Titanic* is marked with a red cross.

stepping stone. Nevertheless, P-B12 is located at 2000 m depth, where currents are slower. As a consequence, the minimum transit time from P-B12 to P1 is 115 days (Fig. 9c) and thus not considerably lower.

3.4.2. *Connectivity between natural occurring populations and the Titanic*

Not all larval particles remain in the LC/DWBC and eventually reach P2. As they encounter the Tail of the Grand Banks, some particles are diverted to the south towards the *Titanic*.

Although larvae can spread and reach the *Titanic* in a relatively short time (within 30 days), there is a large vertical gap between the particles at mid-depth and the *Titanic* at 3800 m depth. Thus, for a connection between the populations to be realized, the larvae must sink due to negative buoyancy, or active downward swimming along the way.

To assess whether this could be possible, we conduct different experiments releasing virtual particles at P1. In these experiment particles can sink at 1.5 mm/s, if they are more than 100 m above the sea floor. Different scenarios were tested in which particles start to sink after a different duration of passive drift. In all scenarios that force particles to stay close to the seafloor very early, they are not advected in the fast LC or main DWBC core, but move with the much slower water at depth and need far longer than 90 days to reach the Tail of the Grand Banks (not shown).

In an experiment with passive drift for 30 days and sinking afterward ($EXP_{P1\text{-}T}$), particles can reach the *Titanic*'s horizontal and vertical vicinity within 50 days. In two of the 12 release months, particles follow the LC/DWBC along the boundary and leave it in an eddying motion at the Tail of the Grand Banks. The velocity snapshot at the time particles leave the western boundary shows an anticyclonic eddy at mid-depth centered at 50.6°W. Due to their added negative velocity, they spiral down the eddy and exactly reach the *Titanic* at approximately the correct depth (Fig. 9d). This is a special case and the vast majority of particles continuously follow the LC/DWBC around the Tail of the Grand Banks, or are diverted into the interior ocean earlier.

Ontogenetic changes in larval buoyancy and behavior are common in deep-sea species (Arellano, 2008; Larsson et al., 2014), but an onset of larval swimming after passive drift of 30 days is unlikely. However, one could also interpret this vertical profile, as larvae becoming negatively buoyant after a certain age and/or their negative buoyancy can be balanced by swimming up to a certain age. However, as mentioned before these experiments are not thought to be a realistic simulation of the true spreading, but help to answer the question, whether closing the vertical gap between the two populations is at least theoretically possible and what larval characteristics would be needed.

Although downstream the DWBC, P-B12 could act as source population of larvae at the wreck site as well, if particles can temporarily spread against the mean flow direction. However, we find that larvae released at P-B12 are strongly confined to the continental slope and exclusively spread in westward direction (Fig. 9c). This is consistent with our hypothesis that the presence of eddies is needed to allow for considerable distances reached against the mean flow. Eddy activity at P-B12 is significantly lower than at the Tail of the Grand Banks.

Since particles from the *Titanic* can spread westward, they reach the vicinity of P-B12 and eventually of P2. As suggested before, without active vertical swimming connectivity from the *Titanic* to P-B12 is not possible, since P-B12 is located further up the continental slope. Because velocities at depth are much lower and particles spread significantly slower the time needed to reach P2 from the *Titanic* well exceeds 90 days. A release experiment from the *Titanic* with an extended run time ($EXP_{T\text{-}P2}$) shows that after 180 days, particles only reach about 57°W (Fig. 9b). Doubling the assumed larval longevity thus only allows larvae

to reach 2° further west (compare Fig. 5). This is caused by particularly slow mean velocities between 53°W and 60°W at depths below 3000 m. Note that there are also no eddies present along the continental slope in this area, that could enhance the flow temporarily. After 300 days (not shown), larval particles can only reach 61°W. Even when larvae (with a large number of stepping stones) could reach 65°W, they arrive at a depth below 3000 m and would need to swim more than 1000 m upwards to reach P2. As a consequence, we conclude that an exchange between the *Titanic* and P2 is not impossible, but unlikely.

In summary, there seems to be a main DWBC pathway that could connect P1 and P2 (with P-B12 as a potential stepping stone). As larvae reach the Tail of the Grand Banks, they can be detrained from the LC/DWBC in eddies and reach the *Titanic*, possibly even without any additional stepping stones. The largest uncertainty, whether such a direct connectivity exists, is the vertical distance between the populations.

From the *Titanic*, the larvae spread westward in a 'deep DWBC' pathway and to the south towards the abyssal ocean. Therefore, the *Titanic* may be a stepping stone from P1 into the abyssal ocean, but likely not a stepping stone from P1 to P2, due to the slow velocities at depths below 3000 m.

Acknowledging that the identification of *C. agassizii* on the wreck was challenged, Fig. 9 also includes the position of known occurrences of all *Chrysogorgia* species from the dataset compiled by Ramiro-Sánchez et al. (2020). However, no additional information about connectivity can be obtained. No additional populations are apparent that may be reached from the *Titanic*, or that could be a source of the *Titanic* population. Populations on the Corner Rise Seamounts at 35°N may be reached from P1 (within 150 days). However, the populations are at a depth of 2000 m and therefore again the larvae would need to bridge a large vertical gap. The southerly pathway away from the *Titanic* is too slow to reach the Corner Rise Seamounts within 180 days once larvae are advected away from the continental slope (Fig. 9b).

4. Summary & discussion

In this study, we investigate whether the natural history legacy of the RMS *Titanic* in abyssal waters depends on upstream connections to distant populations, and whether the *Titanic* herself could now confer a resilience to the network of deep-sea coral populations in the North Atlantic. While the GS is located too far south west of 55°W, the VIKING20X model is able to realistically simulate interactions between the GS and the LC/DWBC close to the wreck site. The magnitude of EKE is overall underestimated compared to observations and ocean reanalysis, in particular along the GS. The vertical structure of EKE compares well with both, direct observations and other models. Also, the strength and vertical structure of the DWBC east of the Grand Banks is realistic. A verification of the models' velocity field at the wreck site is not possible due to the lack of observations. Still, based on the good representation of the mechanism responsible for circulation variability in the region around the *Titanic* and of the mean circulation along the continental slope, we are confident that the study identifies representative dispersal pathways to and from the *Titanic*. This is further supported by the high similarity of trajectories derived from VIKING20X and the GLORYS12 ocean reanalysis and allows us to employ the VIKING20X model to ascertain the importance RMS *Titanic* in today's marine ecosystem connectivity. Below, we summarize and discuss the importance of mesoscale eddies in abyssal and bathyal larval transport, the role of larval biology and limitations in our knowledge, and the contributions the *Titanic* could play in deep-sea coral (as well as other sessile biota) connectivity.

4.1. Mesoscale eddies control dispersal of larvae at the Titanic

In agreement with observations, the circulation above the wreck site in VIKING20X is associated with strong mesoscale eddy activity (Fig. 3). We discover that the position of these mesoscale eddies exerts significant control over the spreading of larvae to and from the RMS *Titanic*. Unexpectedly, effects of mesoscale eddies on dispersal far outweigh effects of either spawning or release season, or larval swimming behavior as defined in our experiments. The mean flow, as well as seasonal to interannual variability, have a minor contribution to the dispersal of larvae (Fig. 5). Instead, our study finds the spreading of *C. agassizii* to and from the RMS *Titanic* to be mainly determined by stochastic processes on subseasonal timescales.

While the eddies have a well-defined structure in the top 1000 m, no closed circulation can be seen at 3800 m. Experiments (EXP_{pas}, EXP_{act} and $EXP_{T\text{-}P2}$) show that larvae seeded at the *Titanic* (at 3800 m) are not entrained into and carried by the closed circulation of the eddies directly. Instead, the abyssal circulation, strongly guided by the bathymetry, responds to the overlying eddies. This leads to a difference between the dominant propagation direction of eddies in this region (south-westward for eddies of subpolar origin and eastward for Gulf Stream rings; Bower et al., 2013; Chelton et al., 2011) to the main spreading direction (westward). Although the mean circulation is directed to the west (Figs. 4 and 6), the presence of mesoscale activity associated with the GS/NAC and LC/DWBC does allow for a faster spreading at certain times, as well as considerable distances reached against the mean flow direction. Additionally, variability of the circulation introduced by eddies allows larvae to cross bottom depth contours, causing a much more diffusive spreading. These results show that the interaction between eddies and the topography can cause very different spreading patterns than expected from the mean flow. As a consequence, the existence of eddies is much more important for larvae spreading away from the *Titanic* than the mean flow (Figs. 5–7). Spreading, not only in the westerly mean flow direction, but additionally to the south, is of particular importance, since it provides a pathway away from the continental slope into the abyssal ocean (Fig. 5). This result is consistent with Wang et al. (2021) who note that in regions where the mean flow dominates, there is little difference between dispersal patterns in annual mean and monthly velocity fields. However, differences become important in the vicinity of topographic features and in the presence of highly variable flows.

Because EKE and the strength of individual eddies at the *Titanic* position are underestimated compared to observations (Fig. 3), the impact of mesoscale activity on the spreading of larvae could be even stronger in the real ocean than described here. Due to the bathymetric constraints a radically different spreading behavior is unlikely, but distances reached from the wreck within 90 days may be larger. One would expect stronger eddies to generate larger anomalies of the circulation at depth that would carry the larvae further away within a given time. Nevertheless, difference between the model, observations and the GLORYS12 reanalysis are most pronounced along the GS axis, while variability of the LC/DWBC is more similar. As the dispersal distance is nearly the same in GLORYS12, this suggests that variability of the LC/DWBC is more important for the dispersal along the continental slope and from the *Titanic* in particular.

Eddies are present nearly everywhere in the ocean (Chelton et al., 2011) and were shown to impact deeper water ecosystem processes including larval dispersal in deep-sea benthic ecosystems. They may help to retain and accumulate deep-sea larvae, or they may help to transport them over long distances. For example, eddy-driven impacts at the northern East Pacific Rise very likely extend beyond the upper ocean and main thermocline and can result in long-distance larval export from the hydrothermal vents (Adams et al., 2011). Other studies find bathymetry, wind variability and currents to results in a deep reaching eddy field that can affect the transport of matter on the seafloor at around 2000 m depth (Wang et al., 2019; Zhang et al., 2014). Our results suggest that an impact of mesoscale variability is not only possible in the upper ocean and mid-depth (e.g., Adams et al., 2011; Bracco et al., 2019), but also at the abyssal depths of the *Titanic*, nearly 4 km deep. Even if the near-surface flow in a given area may not be characterized by particularly strong mesoscale activity, the deep ocean may be (Schulzki

et al., 2021). This highlights the need to perform Lagrangian dispersal experiments in high-resolution models so that simulations can explicitly represent mesoscale eddies and to achieve a more realistic representation of the bathymetry, especially close to the continental slope. Furthermore, eddies occurring at the *Titanic* position are not stationary. In agreement with observations (Bower et al., 2013; Chelton et al., 2011) eddies tend to propagate east, or south-westward, depending on their origin. The modelled velocity fields show that eddies remain above the *Titanic* position for periods shorter than a month. In most other regions of the ocean, eddies are not stationary, but propagate as well (Chelton et al., 2011), suggesting that dispersal studies should be carried out with a temporal resolution of the velocity field below one month to capture the impact of individual eddies.

4.2. The impact of larval behaviors on dispersal from the Titanic wreck

We do not find a significant dependency of the spreading distance or direction of larvae on the season (Fig. 5, Fig. S2). As mesoscale eddies above the *Titanic* position strongly control the spreading, more (or more intense) eddies would need to be present in different seasons to generate a seasonal cycle of the dispersal. A lack of a pronounced seasonal cycle in the modelled EKE is thus consistent with our result and in agreement with Schott et al. (2004), who do not find EKE east of the Grand Banks to show considerable seasonal variations. Whether C. *agassizii* is a seasonal spawner is therefore not expected to strongly affect its potential spreading from the wreck. Dispersal along the upper continental slope (e.g., from P1 to P2), that is mostly determined by coherent currents rather than stochastic eddy variability, could be more strongly affected by the season. The LC was shown to vary substantially between the seasons (Han et al., 2008).

As the vertical velocity shear of individual eddies at abyssal depths is very small (Fig. 8), active swimming to shallower depths with the assumptions regarding duration and speed made in the present study does not greatly alter the dispersal patterns. Vertical swimming has been shown to be favorable for the dispersal of deep-sea species by allowing larvae to reach shallower waters where the circulation is usually faster. Nevertheless, short larval duration and early descent can counteract the advantages of vertical swimming (Gary et al., 2020). The larval duration used for the active experiments of this study is indeed low compared to that of other deep-sea species which display larval duration of several weeks (Hilário et al., 2015; Young et al., 2012), and this may have contributed to the limited role of larval swimming in our study system. On the other hand, some deep-sea species with longer larval duration have different larval characteristics compared to those expected for *C. agassizii*. The deep-sea scleractinian coral *Desmophyllum pertusum* (synonymous with *Lophelia pertusa*), for example, displays larval duration of 3–6 weeks (Larsson et al., 2014), but its larvae are planktotrophic while octocoral larvae are typically lecithotrophic (Waller et al., 2023; Watling et al., 2011). Since there is currently very little knowledge on the larval biology of deep-sea species, we based our experiments on the little information that is currently available for deep-sea octocorals, avoiding comparisons with other taxonomic groups that may display completely different larval traits.

The potential upper limit for the impact of swimming can be derived from $EXP_{P1\text{-}P2}$ and EXP_{B12}. If the PLD is sufficiently long for larvae to reach about 2000 m depth, direct connectivity to P-B12 is possible. At the same time, larvae would get entrained into the main DWBC core with very high current speeds in which they can be transported rapidly towards the Nova Scotian slope (Fig. 9). In this case, they would need to reach about 2000 m depth and stay at this depth to become entrained into the strong DWBC flow.

4.3. Ecosystem connectivity along the Northwest Atlantic continental slope

Larvae released on the continental slope at the eastern side of the Grand Banks (position of population P1; Fig. 2) are rapidly advected southward in the LC/DWBC. A significant number of larvae follow the continental slope and eventually reach a known population off Nova Scotia with one additional stepping stone required (Fig. 9). P-B12 could be such a stepping stone, although due to the greater depth of P-B12 compared to P1, minimum transit times to P2 are similar. As for the spreading of larvae from the *Titanic* itself, the spreading distance from P1 is similar in VIKING20X and the GLORYS12 reanalysis. Our results are further consistent with a study carried out by Wang et al. (2022), who find possible connectivity between corals from the Scotian Shelf to the Tail of the Grand Banks. The larval longevity strongly determines the distance that larvae are transported within the LC/DWBC and thus the number of stepping stones required, again highlighting that further studies on the larval biology of the species are essential.

However, not all virtual larvae continuously follow the LC/DWBC. Some larvae become detrained from the DWBC around the Tail of the Grand Banks and potentially reach the *Titanic* wreck (Fig. 9). Again, mesoscale ocean eddies seem to play a major role. At mid-depth the rotational speed of these eddies is about 6 larger than the translational speed. Thus, consistent with Chelton et al. (2011), eddies can trap and transport particles. As eddies that spin-off from the LC or DWBC predominantly propagate south-westward, larvae can be trapped at the Tail of the Grand Banks and transported toward the *Titanic* position. This in agreement with RAFOS floats leaving the LC and DWBC in eddying motion at nearly the same location, associated with the Labrador Current retroflection (Bower et al., 2013; Gonçalves Neto et al., 2023; Jutras et al., 2023).

Still, there is considerable uncertainty, whether such a connection between P1 and the *Titanic* really exists, since larvae would need to bridge a large vertical gap. We were able to construct an experiment where larvae can reach the *Titanic* within 50 days after release. This experiment requires larvae to bridge the vertical gap by fast downward movement, which could be possible by downward swimming and/or a change in larval buoyancy. Octocoral larvae are typically lecithotrophic, i.e., non-feeding (Watling et al., 2011), and usually contain large reserves in the form of lipids which are also important for larval buoyancy (Arai et al., 1993). During the pelagic phase, consumption of certain lipids like wax esters can indeed lead to a decrease in larval buoyancy (Harii et al., 2007). Regardless of the process, this scenario provides indications of ontogenetic changes in larval behavior after a pelagic phase of at least 30 days, highlighting once again the need for more studies on the larval biology of this species.

Although the general circulation in this area provides a possible connection, the large vertical gap and slower spreading rate at depth make it more likely that connectivity between P1 and *Titanic* is reliant on an intermediary stepping stone with a larval longevity of 90 days. Results obtained by Riehl et al. (2020) and a previously unexplored ridge close to the *Titanic* in 2900 m that is part of Seamount U (Cleland et al., 2024; Pe-Piper et al., 2007; Ocean Gate Expeditions; J.M. Roberts and S. W. Ross, pers. obs.; Fig. 2), suggest that such stepping stones are more frequent than expected. Larvae could reach this recently explored ridge first, which is located about 1000 m shallower than the *Titanic*. This would provide additional scenarios in which larvae could sink at a slower speed.

Nevertheless, a much earlier onset of the downward velocity is unlikely for such a scenario as well. Larvae would still need to be transported in the fast LC/DWBC towards the Tail of the Grand Banks, to reach the Seamount U ridge within a time that does not require the larval longevity to be more than twice our estimate of 90 days. Furthermore, glacial dropstones commonly exist in the North Atlantic, which are attachment sites for deep-sea sessile fauna (Smeulders et al., 2014; Wienberg et al., 2008), but which do not show up on most mapping systems. Compared to the *Titanic* wreck, which constitutes a significant input of hard substrate into a mostly soft-bottomed area, dropstones are much smaller. Therefore, the *Titanic* is more likely to act as a stepping stone for coral dispersal. Still, the existence of dropstones

in the area adds a variety of possible pathways, making connectivity even more probable. Since the positions and suitability of individual dropstones for coral attachments is not known, they can not be included in the connectivity modelling.

It should be noted that the identification of *C. agassizii* on the wreck was challenged (Molodtsova et al., 2008), but considering known natural occurrences of all *Chrysogorgia* species does not allow to infer any other connectivity scenarios involving the *Titanic*.

While active swimming/buoyancy, as defined in our experiment, was found be of minor importance for the spreading from the *Titanic*, it could play a major role for possible sources of larvae at the *Titanic*. Only if swimming capabilities are much higher than expected, they would considerably affect spreading from the *Titanic* itself by allowing direct connectivity to populations along the upper continental slope. A more detailed knowledge of the larvae's buoyancy, swimming behavior and larval longevity, would help to refine our results and better judge, whether the assumptions made here are realistic. Integrated approaches spanning genetics and experimental modelling would give even deeper insights into patterns of connectivity over different temporal and evolutionary timescales (Bracco et al., 2019).

As described before, from the *Titanic*, larvae may be exported along southern and westerly pathways further into the abyss. While experiments indicated that the *Titanic* is unlikely a direct source of *C. agassizii* larvae for already known populations (Figs. 5 and 9) along the Northwest Atlantic continental slope, the wreck possibly functions as a stepping stone, connecting coral populations from the slopes of the Grand Banks to abyssal populations in ABNJ along westerly and southerly circulation pathways.

With a slightly longer larval longevity than 90 days, or the ability of larvae to swim upwards, it is possible that larvae can directly reach the Canadian EEZ. Especially in combination with a longer PLD than 6 days, vertical swimming could greatly increase the number of living larvae that arrives in the EEZ. Furthermore, additional stepping stones in between would enhance the likeliness of larvae in the EEZ being supplied by the *Titanic*.

5. Conclusion: The *Titanic*'s role in ecosystem connectivity and the importance of eddies

Depending on larval buoyancy, duration and the configuration of stepping stones, ocean circulation provides several possible pathways for larvae from a natural occurring population on the eastern slope of the Grand Banks to reach the *Titanic*, despite a large vertical gap. The interaction of eddies with the bathymetry generates two pathways away from the *Titanic*, allowing larvae to reach the Canadian EEZ along the deep continental slope, and to spread away from the slope into the abyssal North Atlantic. Therefore, the transboundary nature of coral dispersal to and from the *Titanic* is interesting on both geopolitical and ecological levels. Canada may in the future have jurisdictional rights over the *Titanic* through its claim to extend its EEZ, through which it could afford specific conservation measures, e.g., establishing a marine protected area to protect an important stepping stone for vulnerable deep-sea corals. Based on unknown larval characteristics and model uncertainties, there are different scenarios of this dispersal and the resulting connectivity in the Northwest Atlantic, but all converge on the role of Titanic as some sort of stepping stone. Although it was concluded that the model is able to capture the correct mechanisms responsible for variability above the wreck site and an overall realistic deep circulation, direct observations of the velocity field at abyssal depths would be essential to verify that the model correctly simulates the circulation at the wreck site. Therefore, this study provides further motivation to study the highly complex oceanographic conditions at the Tail of the Grand Banks and their impact on the abyssal circulation. Our experiments also provide useful information, which biological and physical parameters must be known to narrow down the possible pathways from and to the *Titanic* discussed here. In any case and given the findings of the present study, it is unlikely that the *Titanic* is completely isolated from known or unknown populations of *C. agassizii*. While we have focused on a *C. agassizii* for this study, many results are valid for other marine species as well.

Similarly, our study was motivated by a specific case, the wreck of the RMS *Titanic*, but our findings can also be generalized to other regions of the world oceans. They support the importance of deep mesoscale eddies and fine-scale structures to understand the connectivity between deep ecosystems. Eddying structures can easily enhance or compensate the usually weaker mean flow, and in combination with bathymetry, lead to pronounced unidirectional dispersal patterns. High-resolution ocean modelling is required to correctly simulate the corresponding ocean dynamics. It can also provide answers on the importance of potentially unknown swimming or buoyancy motions of deep-sea organisms.

CRediT authorship contribution statement

Tobias Schulzki: Writing – review & editing, Writing – original draft, Visualization, Methodology, Formal analysis, Conceptualization. **Lea-Anne Henry:** Writing – review & editing, Writing – original draft, Methodology, Conceptualization. **J. Murray Roberts:** Writing – review & editing, Methodology, Conceptualization. **Maria Rakka:** Writing – review & editing, Writing – original draft, Methodology. **Steve W. Ross:** Writing – review & editing. **Arne Biastoch:** Writing – review & editing, Supervision, Methodology, Funding acquisition, Conceptualization.

Declaration of competing interest

The authors declare that they have no known competing financial interests or personal relationships that could have appeared to influence the work reported in this paper.

Data availability

Derived data and scripts are available at https://hdl.handle.net/20.500.12085/f2abbdc6-e81a-45b5-afb8-feecb33e10b3 (Schulzki et al., 2023). The full model output is available through the World Data Center for Climate (Getzlaff et al., 2024).

Acknowledgements

This study has received funding from the European Union's Horizon 2020 research and innovation programme under grant agreement No. 818123 for the iAtlantic project. This output reflects only the authors' views and the European Union cannot be held responsible for any use that may be made of the information contained therein. This research was supported in part through high-performance computing resources available at the Kiel University Computing Centre. The ocean model simulation was performed at the North-German Supercomputing Alliance (HLRN). We thank OceanGate Expeditions for providing access to recent (2021 and 2022) submersible observations and data about the *Titanic* site and Seamount U ridge. ANDRO argo floats displacements product is made freely available by SNO Argo France at LOPS Laboratory (supported by UBO/CNRS/Ifremer/IRD) and IUEM Observatory (OSU IUEM/CNRS/INSU), and was funded by Ifremer, Coriolis, SOERE-CTDO2 and SNO Argo France at doi: https://doi.org/10.17882/47077. The Ssalto/Duacs altimeter products and GLORYS12v1 ocean reanalysis were distributed by the Copernicus Marine and Environment Monitoring Service (CMEMS), https://marine.copernicus.eu/. We thank 3 anonymous reviewers for their constructive comments during the review process.

Appendix A. Supplementary data

Supplementary data to this article can be found online at https://doi.

org/10.1016/j.dsr.2024.104404.

References

Adams, D.K., McGillicuddy, D.J., Zamudio, L., Thurnherr, A.M., Liang, X., Rouxel, O., German, C.R., Mullineaux, L.S., 2011. Surface-generated mesoscale eddies transport deep-sea products from hydrothermal vents. Science 332, 580–583. https://doi.org/10.1126/science.1201066.

Arai, I., Kato, M., Heyward, A., Ikeda, Y., Iizuka, T., Maruyama, T., 1993. Lipid composition of positively buoyant eggs of reef building corals. Coral Reefs 12, 71–75. https://doi.org/10.1007/BF00302104.

Arakawa, A., Hsu, Y.-J.G., 1990. Energy conserving and potential-enstrophy dissipating schemes for the shallow water equations. Mon. Weather Rev. 118, 1960–1969. https://doi.org/10.1175/1520-0493(1990)118<1960:ECAPED>2.0.CO;2.

Arellano, S.M., 2008. Embryology, larval ecology, and recruitment of. "Bathymodiolus" Childressi, a Cold-Seep Mussel from the Gulf of Mexico (Ph.D. Thesis). University of Oregon.

Aznar, M.J., Varmer, O., 2013. The titanic as underwater cultural heritage: challenges to its legal international protection. Ocean Dev. Int. Law 44, 96–112. https://doi.org/10.1080/00908320.2013.750978.

Baena, P., Martell, L., Soto-Angel, J.J., Ambroso, S., López-González, P.J., 2024. A new deep-sea species of golden gorgonian (Octocorallia: Scleralcyonacea: Chrysogorgiidae) from Antarctic waters. Deep-Sea Res. I: Oceanogr. Res. Pap. 204, 104234. https://doi.org/10.1016/j.dsr.2024.104234.

Baker, K.D., Wareham, V.E., Snelgrove, P.V.R., Haedrich, R.L., Fifield, D.A., Edinger, E. N., Gilkinson, K.D., 2012. Distributional patterns of deep-sea coral assemblages in three submarine canyons off Newfoundland, Canada. Mar. Ecol. Prog. Ser. 445, 235–249.

Barnier, B., Madec, G., Penduff, T., Molines, J.-M., Treguier, A.-M., Le Sommer, J., Beckmann, A., Biastoch, A., Böning, C., Dengg, J., Derval, C., Durand, E., Gulev, S., Remy, E., Talandier, C., Theetten, S., Maltrud, M., McClean, J., Cuevas, B., 2006. Impact of partial steps and momentum advection schemes in a global ocean circulation model at eddy-permitting resolution. Ocean Dynam. 56, 543–567. https://doi.org/10.1007/s10236-006-0082-1.

Beaulieu, S.E., Sayre-McCord, R.T., Mills, S.W., Pradillon, F., Watanabe, H., 2015. Swimming speeds of polychaete larvae collected near deep-sea hydrothermal vents. Mar. Ecol. 36, 133–143. https://doi.org/10.1111/maec.12207.

Ben-David-Zaslow, R., Benayahu, Y., 1998. Competence and longevity in planulae of several species of soft corals. Mar. Ecol. Prog. Ser. 163, 235–243.

Biastoch, A., Schwarzkopf, F.U., Getzlaff, K., Rühs, S., Martin, T., Scheinert, M., Schulzki, T., Handmann, P., Hummels, R., Böning, C.W., 2021. Regional imprints of changes in the atlantic meridional overturning circulation in the eddy-rich ocean model VIKING20X. Ocean Sci. Discuss. 2021, 1–52. https://doi.org/10.5194/os-2021-37.

Blanke, B., Bonhommeau, S., Grima, N., Drillet, Y., 2012. Sensitivity of advective transfer times across the North Atlantic Ocean to the temporal and spatial resolution of model velocity data: implication for European eel larval transport. Dynam. Atmos. Oceans 55–56, 22–44. https://doi.org/10.1016/j.dynatmoce.2012.04.003.

Bonhommeau, S., Blanke, B., Tréguier, A.-M., Grima, N., Rivot, E., Vermard, Y., Greiner, E., Le Pape, O., 2009. How fast can the European eel (Anguilla anguilla) larvae cross the Atlantic Ocean? Fish. Oceanogr. 18, 371–385. https://doi.org/10.1111/j.1365-2419.2009.00517.x.

Bower, A., Lozier, S., Gary, S., 2011. Export of Labrador Sea water from the subpolar North Atlantic: a Lagrangian perspective. Deep Sea Res. Part II Top. Stud. Oceanogr. 58, 1798–1818. https://doi.org/10.1016/j.dsr2.2010.10.060.

Bower, A.S., Hendry, R.M., Amrhein, D.E., Lilly, J.M., 2013. Direct observations of formation and propagation of subpolar eddies into the Subtropical North Atlantic. Deep Sea Res. Part II Top. Stud. Oceanogr. 85, 15–41. https://doi.org/10.1016/j.dsr2.2012.07.029.

Bower, A.S., Lozier, M.S., Gary, S.F., Böning, C.W., 2009. Interior pathways of the North Atlantic meridional overturning circulation. Nature 459, 243–247. https://doi.org/10.1038/nature07979.

Bracco, A., Liu, G., Galaska, M.P., Quattrini, A.M., Herrera, S., 2019. Integrating physical circulation models and genetic approaches to investigate population connectivity in deep-sea corals. J. Mar. Syst. 198, 103189. https://doi.org/10.1016/j.jmarsys.2019.103189.

Breusing, C., Biastoch, A., Drews, A., Metaxas, A., Jollivet, D., Vrijenhoek, R.C., Bayer, T., Melzner, F., Sayavedra, L., Petersen, J.M., Dubilier, N., Schilhabel, M.B., Rosenstiel, P., Reusch, T.B.H., 2016. Biophysical and population genetic models predict the presence of "phantom" stepping stones connecting mid-atlantic ridge vent ecosystems. Curr. Biol. 26, 2257–2267. https://doi.org/10.1016/j.cub.2016.06.062.

Brickman, D., Hebert, D., Wang, Z., 2018. Mechanism for the recent ocean warming events on the Scotian Shelf of eastern Canada. Continent. Shelf Res. 156, 11–22. https://doi.org/10.1016/j.csr.2018.01.001.

Bright, D.A., Williams, R.M.L., McLare, A.S., 2005. Comparative photometric analysis of structural degradation on the bow of RMS Titanic. In: Proceedings of OCEANS 2005 MTS/IEEE. Presented at the Proceedings of OCEANS 2005 MTS/IEEE, vol. 1, pp. 106–110. https://doi.org/10.1109/OCEANS.2005.1639746.

Brown, O.B., Cornillon, P.C., Emmerson, S.R., Carle, H.M., 1986. Gulf Stream warm rings: a statistical study of their behavior. Deep Sea Research Part A. Oceanographic Res. Papers 33, 1459–1473. https://doi.org/10.1016/0198-0149(86)90062-2.

Busch, K., Taboada, S., Riesgo, A., Koutsouveli, V., Ríos, P., Cristobo, J., Franke, A., Getzlaff, K., Schmidt, C., Biastoch, A., Hentschel, U., 2021. Population connectivity of fan-shaped sponge holobionts in the deep Cantabrian Sea. Deep Sea Res. Oceanogr. Res. Pap. 167, 103427. https://doi.org/10.1016/j.dsr.2020.103427.

Cairns, S.D., 2001. Studies on western Atlantic Octocorallia (Coelenterata: Anthozoa) Part 1: the genus Chrysogorgia Duchassaing & Michelotti, 1864. Proc. Biol. Soc. Wash. 114 (3), 746–787.

Chelton, D.B., Schlax, M.G., Samelson, R.M., 2011. Global observations of nonlinear mesoscale eddies. Prog. Oceanogr. 91, 167–216. https://doi.org/10.1016/j.pocean.2011.01.002.

Chelton, D.B., Schlax, M.G., Samelson, R.M., de Szoeke, R.A., 2007. Global observations of large oceanic eddies. Geophys. Res. Lett. 34. https://doi.org/10.1029/2007GL030812.

Cleland, J., Gebruk, A., Roberts, J.M., Aleynik, D., McClenaghan, B., Hajibabaei, M., Mather, R., Buxton, B., Ross, S.W., 2024. Megafauna of the RMS *Titanic* shipwreck and an unexplored seamount ridge in the deep sea of the Western North Atlantic. Mauscript in submission to Deep-Sea Research Part I.

Coelho, M.A.G., Lasker, H.R., 2016. Larval behavior and settlement dynamics of a ubiquitous Caribbean octocoral and its implications for dispersal. Mar. Ecol. Prog. Ser. 561, 109–121.

Copernicus Marine Service Information (CMEMS), 2023. GLORYS12V1 global ocean physics reanalysis. Marine Data Store (MDS). https://doi.org/10.48670/moi-00021.

Cullimore, D.R., Johnston, L.A., 2008. Microbiology of concretions, sediments and mechanisms influencing the preservation of submerged archaeological artifacts. Int. J. Hist. Archaeol. 12, 120–132. https://doi.org/10.1007/s10761-008-0045-y.

Daniault, N., Mercier, H., Lherminier, P., Sarafanov, A., Falina, A., Zunino, P., Pérez, F.F., Ríos, A.F., Ferron, B., Huck, T., Thierry, V., Gladyshev, S., 2016. The northern North Atlantic Ocean mean circulation in the early 21st century. Prog. Oceanogr. 146, 142–158. https://doi.org/10.1016/j.pocean.2016.06.007.

De Verdière, A.C., Merchier, H., Arhan, M., 1989. Mesoscale variability transition from the western to the eastern atlantic along 48°N. J. Phys. Oceanogr. 19, 1149–1170. https://doi.org/10.1175/1520-0485(1989)019<1149:MVTFTW>2.0.CO;2.

Debreu, L., Vouland, C., Blayo, E., 2008. AGRIF: Adaptive grid refinement in Fortran. Comput. Geosci. 34, 8–13. https://doi.org/10.1016/j.cageo.2007.01.009.

Delandmeter, P., van Sebille, E., 2019. The Parcels v2.0 Lagrangian framework: new field interpolation schemes. Geosci. Model Dev. (GMD) 12, 3571–3584. https://doi.org/10.5194/gmd-12-3571-2019.

Ducet, N., Le Traon, P.-Y., 2001. A comparison of surface eddy kinetic energy and Reynolds stresses in the Gulf Stream and the Kuroshio Current systems from merged TOPEX/Poseidon and ERS-1/2 altimetric data. J. Geophys. Res.: Oceans 106, 16603–16622. https://doi.org/10.1029/2000JC000205.

Ducousso, N., Le Sommer, J., Molines, J.-M., Bell, M., 2017. Impact of the "symmetric instability of the computational kind" at mesoscale- and submesoscale-permitting resolutions. Ocean Model. 120, 18–26. https://doi.org/10.1016/j.ocemod.2017.10.006.

Fichefet, T., Maqueda, M.A.M., 1997. Sensitivity of a global sea ice model to the treatment of ice thermodynamics and dynamics. J. Geophys. Res.: Oceans 102, 12609–12646. https://doi.org/10.1029/97JC00480.

Flanders Marine Institute, 2019. Maritime boundaries geodatabase. version 11. https://doi.org/10.14284/382.

Fontoura, L., D'Agata, S., Gamoyo, M., Barneche, D.R., Luiz, O.J., Madin, E.M.P., Eggertsen, L., Maina, J.M., 2022. Protecting connectivity promotes successful biodiversity and fisheries conservation. Science 375, 336–340. https://doi.org/10.1126/science.abg4351.

Fratantoni, P.S., McCartney, M.S., 2010. Freshwater export from the labrador current to the North atlantic current at the Tail of the Grand Banks of Newfoundland. Deep Sea Res. Oceanogr. Res. Pap. 57, 258–283. https://doi.org/10.1016/j.dsr.2009.11.006.

Frazão, H.C., Prien, R.D., Schulz-Bull, D.E., Seidov, D., Waniek, J.J., 2022. The forgotten Azores current: a long-term perspective. Front. Mar. Sci. 9.

Gary, S.F., Fox, A.D., Biastoch, A., Roberts, J.M., Cunningham, S.A., 2020. Larval behaviour, dispersal and population connectivity in the deep sea. Sci. Rep. 10, 10675. https://doi.org/10.1038/s41598-020-67503-7.

Getzlaff, K., Schwarzkopf, F.U.. *VIKING20X-JRA-short: daily to multi-decadal ocean dynamics under JRA55-do atmospheric forcing*. World Data Center for Climate (WDCC) at DKRZ. https://doi.org/10.26050/WDCC/VIKING20XJRAshort.

Gonçalves Neto, A., Palter, J.B., Xu, X., Fratantoni, P., 2023. Temporal variability of the labrador current pathways around the Tail of the Grand Banks at intermediate depths in a high-resolution ocean circulation model. J. Geophys. Res.: Oceans 128, e2022JC018756. https://doi.org/10.1029/2022JC018756.

Gravina, M.F., Casoli, E., Donnarumma, L., Giampaoletti, J., Antonelli, F., Sacco Perasso, C., Ricci, S., 2021. First report on the benthic invertebrate community associated with a Bronze Naval Ram from the first punic war: a proxy of marine biodiversity. Front. Mar. Sci. 8.

Griffies, S.M., Biastoch, A., Böning, C., Bryan, F., Danabasoglu, G., Chassignet, E.P., England, M.H., Gerdes, R., Haak, H., Hallberg, R.W., Hazeleger, W., Jungclaus, J., Large, W.G., Madec, G., Pirani, A., Samuels, B.L., Scheinert, M., Gupta, A.S., Severijns, C.A., Simmons, H.L., Treguier, A.M., Winton, M., Yeager, S., Yin, J., 2009. Coordinated Ocean-Ice reference experiments (COREs). Ocean Model. 26, 1–46. https://doi.org/10.1016/j.ocemod.2008.08.007.

Guizien, K., Viladrich, N., Martínez-Quintana, Á., Bramanti, L., 2020. Survive or swim: different relationships between migration potential and larval size in three sympatric Mediterranean octocorals. Sci. Rep. 10, 18096. https://doi.org/10.1038/s41598-020-75099-1.

Guy, G., Metaxas, A., 2022. Recruitment of deep-water corals and sponges in the Northwest Atlantic Ocean: implications for habitat distribution and population connectivity. Mar. Biol. 169. https://doi.org/10.1007/s00227-022-04089-w.

Hamdan, L.J., Hampel, J.J., Moseley, R.D., Mugge, RachelL., Ray, A., Salerno, J.L., Damour, M., 2021. Deep-sea shipwrecks represent island-like ecosystems for marine

microbiomes. ISME J. 15, 2883–2891. https://doi.org/10.1038/s41396-021-00978-y.
Han, G., Lu, Z., Wang, Z., Helbig, J., Chen, N., de Young, B., 2008. Seasonal variability of the labrador current and shelf circulation off Newfoundland. J. Geophys. Res.: Oceans 113. https://doi.org/10.1029/2007JC004376.
Handmann, P., Fischer, J., Visbeck, M., Karstensen, J., Biastoch, A., Böning, C., Patara, L., 2018. The deep western boundary current in the Labrador Sea from observations and a high-resolution model. J. Geophys. Res.: Oceans 123, 2829–2850. https://doi.org/10.1002/2017JC013702.
Harii, S., Nadaoka, K., Yamamoto, M., Iwao, K., 2007. Temporal changes in settlement, lipid content and lipid composition of larvae of the spawning hermatypic coral Acropora tenuis. Mar. Ecol. Prog. Ser. 346, 89–96.
Hilário, A., Metaxas, A., Gaudron, S.M., Howell, K.L., Mercier, A., Mestre, N.C., Ross, R. E., Thurnherr, A.M., Young, C., 2015. Estimating dispersal distance in the deep sea: challenges and applications to marine reserves. Front. Mar. Sci. 2.
Jutras, M., Dufour, C.O., Mucci, A., Talbot, L.C., 2023. Large-scale control of the retroflection of the labrador current. Nat. Commun. 14, 2623. https://doi.org/10.1038/s41467-023-38321-y.
Kenchington, E., Wang, Z., Lirette, C., Murillo, F.J., Guijarro, J., Yashayaev, I., Maldonado, M., 2019. Connectivity modelling of areas closed to protect vulnerable marine ecosystems in the northwest Atlantic. Deep Sea Res. Oceanogr. Res. Pap. 143, 85–103. https://doi.org/10.1016/j.dsr.2018.11.007.
Large, W.G., Yeager, S.G., 2009. The global climatology of an interannually varying air–sea flux data set. Clim. Dynam. 33, 341–364. https://doi.org/10.1007/s00382-008-0441-3.
Larsson, A.I., Järnegren, J., Strömberg, S.M., Dahl, M.P., Lundälv, T., Brooke, S., 2014. Embryogenesis and larval biology of the cold-water coral Lophelia pertusa. PLoS One 9, e102222. https://doi.org/10.1371/journal.pone.0102222.
Le Corre, N., Pepin, P., Snelgrove, P., 2018. Connectivity of bentho-pelagic species among significant benthic areas off Newfoundland and labrador. Zenodo. https://doi.org/10.5281/zenodo.1255743.
Lecours, V., Gábor, L., Edinger, E., Devillers, R., 2020. Chapter 44 - fine-scale habitat characterization of the gully, the flemish Cap, and the orphan knoll, Northwest Atlantic, with a focus on cold-water corals. In: Harris, P.T., Baker, E. (Eds.), Seafloor Geomorphology as Benthic Habitat, second ed. Elsevier, pp. 735–751. https://doi.org/10.1016/B978-0-12-814960-7.00044-0.
Lellouche, J.-M., Blair, E., Bourdallé-Badie, R., Garric, G., Melet, A., Drévillon, M., Bricaud, C., Hamon, M., Le Galloudec, O., Regnier, C., Candela, T., Testut, C.-E., Gasparin, F., Ruggiero, G., Benkiran, M., Drillet, Y., Le Traon, P.-Y., 2021. The Copernicus global 1/12° oceanic and sea ice GLORYS12 reanalysis. Front. Earth Sci. 9.
Martin, J.B., 2018. Protecting outstanding underwater cultural heritage through the world heritage Convention: the titanic and Lusitania as world heritage sites. Int. J. Mar. Coast. Law 33, 116–165. https://doi.org/10.1163/15718085-13301069.
Martínez-Quintana, A., Bramanti, L., Viladrich, N., Rossi, S., Guizien, K., 2015. Quantification of larval traits driving connectivity: the case of Corallium rubrum (L. 1758). Mar. Biol. 162, 309–318. https://doi.org/10.1007/s00227-014-2599-z.
Meredyk, S.P., Edinger, E., Piper, D.J.W., Huvenne, V.A.I., Hoy, S., Ruffman, A., 2020. Enigmatic deep-water mounds on the Orphan Knoll, Labrador Sea. Front. Mar. Sci. 6.
Mertens, C., Rhein, M., Walter, M., Böning, C.W., Behrens, E., Kieke, D., Steinfeldt, R., Stöber, U., 2014. Circulation and transports in the Newfoundland Basin, western subpolar North Atlantic. J. Geophys. Res.: Oceans 119, 7772–7793. https://doi.org/10.1002/2014JC010019.
Mertens, C., Roessler, A., Rhein, M., 2019. Lowered ADCP Data in the Western Subpolar North Atlantic (47°N). PANGAEA. https://doi.org/10.1594/PANGAEA.903209.
Metaxas, A., Lacharité, M., de Mendonça, S.N., 2019. Hydrodynamic connectivity of habitats of deep-water corals in Corsair Canyon, Northwest Atlantic: a case for cross-boundary conservation. Front. Mar. Sci. https://doi.org/10.3389/fmars.2019.00159.
Meyer-Kaiser, K.S., Mires, C.H., 2022. Underwater cultural heritage is integral to marine ecosystems. Trends Ecol. Evol. 37, 815–818. https://doi.org/10.1016/j.tree.2022.06.014.
Molodtsova, T.N., Sanamyan, N.P., Keller, N.B., 2008. Anthozoa from the northern mid-Atlantic Ridge and Charlie-Gibbs Fracture Zone. Mar. Biol. Res. 4, 112–130. https://doi.org/10.1080/17451000701821744.
Morato, T., González-Irusta, J.-M., Dominguez-Carrió, C., Wei, C.-L., Davies, A., Sweetman, A.K., Taranto, G.H., Beazley, L., García-Alegre, A., Grehan, A., Laffargue, P., Murillo, F.J., Sacau, M., Vaz, S., Kenchington, E., Arnaud-Haond, S., Callery, O., Chimienti, G., Cordes, E., Egilsdottir, H., Freiwald, A., Gasbarro, R., Gutiérrez-Zárate, C., Gianni, M., Gilkinson, K., Wareham Hayes, V.E., Hebbeln, D., Hedges, K., Henry, L.-A., Johnson, D., Koen-Alonso, M., Lirette, C., Mastrototaro, F., Menot, L., Molodtsova, T., Durán Muñoz, P., Orejas, C., Pennino, M.G., Puerta, P., Ragnarsson, S.Á., Ramiro-Sánchez, B., Rice, J., Rivera, J., Roberts, J.M., Ross, S.W., Rueda, J.L., Sampaio, Í., Snelgrove, P., Stirling, D., Treble, M.A., Urra, J., Vad, J., van Oevelen, D., Watling, L., Walkusz, W., Wienberg, C., Woillez, M., Levin, L.A., Carreiro-Silva, M., 2020. Climate-induced changes in the suitable habitat of cold-water corals and commercially important deep-sea fishes in the North Atlantic. Global Change Biol. 26, 2181–2202. https://doi.org/10.1111/gcb.14996.
Müller, V., Kieke, D., Myers, P.G., Pennelly, C., Steinfeldt, R., Stendardo, I., 2019. Heat and freshwater transport by mesoscale eddies in the southern subpolar North Atlantic. J. Geophys. Res.: Oceans 124, 5565–5585. https://doi.org/10.1029/2018JC014697.
New, A.L., Smeed, D.A., Czaja, A., Blaker, A.T., Mecking, J.V., Mathews, J.P., Sanchez-Franks, A., 2021. Labrador slope water connects the subarctic with the Gulf Stream. Environ. Res. Lett. 16, 084019. https://doi.org/10.1088/1748-9326/ac1293.
Ollitrault, M., Rannou, P., Brion, E., Cabanes, C., Piron, A., Reverdin, G., Kolodziejczyk, N., 2022. ANDRO: an Argo-Based Deep Displacement Dataset, SEANOE. https://doi.org/10.17882/47077.
Pante, E., France, S.C., Couloux, A., Cruaud, C., McFadden, C.S., Samadi, S., Watling, L., 2012. Deep-Sea origin and in-situ diversification of chrysogorgiid octocorals. PLoS One 7, e38357. https://doi.org/10.1371/journal.pone.0038357.
Paxton, A.B., Blair, E., Blawas, C., Fatzinger, M.H., Marens, M., Holmberg, J., Kingen, C., Houppermans, T., Keusenkothen, M., McCord, J., Silliman, B.R., Penfold, L.M., 2019. Citizen science reveals female sand tiger sharks (Carcharias taurus) exhibit signs of site fidelity on shipwrecks. Ecology 100, 1–4.
Pe-Piper, G., Piper, D.J., Jansa, L.F., De Jonge, A., 2007. Early Cretaceous opening of the North Atlantic Ocean: Implications of the petrology and tectonic setting of the Fogo Seamounts off the SW Grand Banks, Newfoundland. Geol. Soc. Am. Bull. 119, 712–724.
Ragnarsson, S.Á., Burgos, J.M., Kutti, T., van den Beld, I., Egilsdóttir, H., Arnaud-Haond, S., Grehan, A., 2017. The impact of anthropogenic activity on cold-water corals. In: Rossi, S., Bramanti, L., Gori, A., Orejas, C. (Eds.), Marine Animal Forests: the Ecology of Benthic Biodiversity Hotspots. Springer International Publishing, Cham, pp. 989–1023. https://doi.org/10.1007/978-3-319-21012-4_27.
Rakka, M., 2021. Cold-water Corals in a Changing World: Potential Impacts of Climate Change across Coral Life History Stages. University of the Azores. PhD Dissertation, University of the Azores (Ph.D. Thesis).
Rakka, M., Godinho, A., Orejas, C., Carreiro-Silva, M., 2021. Embryo and larval biology of the deep-sea octocoral Dentomuricea aff. meteor under different temperature regimes. PeerJ 9. https://doi.org/10.7717/peerj.11604.
Ramiro-Sánchez, B., Henry, L.-A., Morato, T., Taranto, G., Cleland, J., Carreiro-Silva, M., Sampaio, Í., Domínguez-Carrió, C., Messing, C.G., Kenchington, E.L., Murton, B., Roberts, J.M., 2020. Compilation of records of vulnerable marine ecosystem indicator taxa in the North Atlantic. https://doi.org/10.1594/PANGAEA.920658.
Rhein, M., Mertens, C., Roessler, A., 2019. Observed transport decline at 47°N, western atlantic. J. Geophys. Res.: Oceans 124, 4875–4890. https://doi.org/10.1029/2019JC014993.
Richardson, P.L., 1983. A vertical section of eddy kinetic energy through the Gulf Stream system. J. Geophys. Res.: Oceans 88, 2705–2709. https://doi.org/10.1029/JC088iC04p02705.
Richardson, P.L., Maillard, C., Stanford, T.B., 1979. The physical structure and life history of cyclonic Gulf Stream Ring Allen. J. Geophys. Res.: Oceans 84, 7727–7741. https://doi.org/10.1029/JC084iC12p07727.
Rieck, J.K., Böning, C.W., Getzlaff, K., 2019. The nature of eddy kinetic energy in the Labrador Sea: different types of mesoscale eddies, their temporal variability, and impact on deep convection. J. Phys. Oceanogr. 49, 2075–2094. https://doi.org/10.1175/JPO-D-18-0243.1.
Riehl, T., Wölfl, A.-C., Augustin, N., Devey, C.W., Brandt, A., 2020. Discovery of widely available abyssal rock patches reveals overlooked habitat type and prompts rethinking deep-sea biodiversity. Proc. Natl. Acad. Sci. USA 117, 15450–15459. https://doi.org/10.1073/pnas.1920706117.
Roberts, J.M., Devey, C.W., Biastoch, A., Carreiro-Silva, M., Dohna, T., Dorschel, B., Gunn, V., Al Huvenne, V., Johnson, D.E., Jollivet, D., Kenchington, E., Larkin, K., Matabos, M., Morato, T., Naumann, M.S., Orejas, C., Perez, J.A., Ragnarsson, S.A., Smit, A.J., Sweetman, A., Unger, S., Boteler, B., Henry, L.-A., 2022. A blueprint for integrating scientific approaches and international communities to assess basin-wide ocean ecosystem status. Nat. Commun. Earth Environ (in press).
Ross, R.E., Nimmo-Smith, W.A.M., Torres, R., Howell, K.L., 2020. Comparing deep-sea larval dispersal models: a cautionary tale for ecology and conservation. Front. Mar. Sci. 7.
Ross, S.W., Rhode, M., Viada, S.T., Mather, R., 2016. Fish species associated with shipwreck and natural hard-bottom habitats from the middle to outer continental shelf of the Middle Atlantic Bight near Norfolk Canyon. Fish. Bull. 114, 45–57. https://doi.org/10.7755/FB.114.1.4.
Rühs, S., Oliver, E.C.J., Biastoch, A., Böning, C.W., Dowd, M., Getzlaff, K., Martin, T., Myers, P.G., 2021. Changing spatial patterns of deep convection in the subpolar North Atlantic. J. Geophys. Res.: Oceans 126, e2021JC017245. https://doi.org/10.1029/2021JC017245.
Rühs, S., Zhurbas, V., Koszalka, I.M., Durgadoo, J.V., Biastoch, A., 2018. Eddy diffusivity estimates from Lagrangian trajectories simulated with ocean models and surface drifter data—a case study for the greater agulhas system. J. Phys. Oceanogr. 48, 175–196. https://doi.org/10.1175/JPO-D-17-0048.1.
Salazar, M., Little, B., 2017. Review: rusticle formation on the RMS titanic and the potential influence of oceanography. J. Marit. Archaeol. 12, 25–32. https://doi.org/10.1007/s11457-016-9168-1.
Saunders, P.M., 1971. Anticyclonic eddies formed from shoreward meanders of the Gulf Stream. Deep Sea Res. Oceanogr. Abstr. 18, 1207–1219. https://doi.org/10.1016/0011-7471(71)90027-1.
Schott, F.A., Zantopp, R., Stramma, L., Dengler, M., Fischer, J., Wibaux, M., 2004. Circulation and deep-water export at the western exit of the subpolar North Atlantic. J. Phys. Oceanogr. 34, 817–843. https://doi.org/10.1175/1520-0485(2004)034<0817:CADEAT>2.0.CO;2.
Schubert, R., Biastoch, A., Cronin, M.F., Greatbatch, R.J., 2018. Instability-driven benthic storms below the separated Gulf Stream and the North atlantic current in a high-resolution ocean model. J. Phys. Oceanogr. 48, 2283–2303. https://doi.org/10.1175/JPO-D-17-0261.1.
Schulzki, T., Getzlaff, K., Biastoch, A., 2021. On the variability of the DWBC transport between 26.5°N and 16°N in an eddy-rich ocean model. J. Geophys. Res.: Oceans 126, e2021JC017372. https://doi.org/10.1029/2021JC017372.
Schulzki, T., Henry, L.-A., Roberts, J.M., Rakka, M., Ross, S.W., Biastoch, A., 2023. Mesoscale ocean eddies determine dispersal and connectivity of corals at the RMS

Titanic wreck site [dataset]. GEOMAR Helmholtz Centre for Ocean Research Kiel [distributor]. hdl:20.500.12085/f2abbdc6-e81a-45b5-afb8-feecb33e10b3.
Seidov, D., Mishonov, A., Reagan, J., Parsons, R., 2019. Resilience of the Gulf Stream path on decadal and longer timescales. Sci. Rep. 9, 11549. https://doi.org/10.1038/s41598-019-48011-9.
Shay, T.J., Bane, J.M., Watts, D.R., Tracey, K.L., 1995. Gulf Stream flow field and events near 68°W. J. Geophys. Res.: Oceans 100, 22565–22589. https://doi.org/10.1029/95JC02685.
Smeulders, G.G.B., Koho, K.A., de Stigter, H.C., Mienis, F., de Haas, H., van Weering, T.C. E., 2014. Cold-water coral habitats of rockall and porcupine bank, NE Atlantic Ocean: sedimentary facies and benthic foraminiferal assemblages. Deep Sea Res. Part II Top. Stud. Oceanogr. 99, 270–285. https://doi.org/10.1016/j.dsr2.2013.10.001.
Smith, R.D., Maltrud, M.E., Bryan, F.O., Hecht, M.W., 2000. Numerical simulation of the North Atlantic Ocean at 1/10. J. Phys. Oceanogr. 30, 1532–1561. https://doi.org/10.1175/1520-0485(2000)030<1532:NSOTNA>2.0.CO;2.
Sun, Z., Hamel, J.F., Mercier, A., 2010. Planulation periodicity, settlement preferences and growth of two deep-sea octocorals from the northwest Atlantic. Mar. Ecol. Prog. Ser. 410, 71–87.
Taburet, G., Pujol, M.-I., 2022. Global Ocean gridded L 4 Sea Surface heights and derived variables reprocessed Copernicus climate service. Copernicus Climate Change Service. https://doi.org/10.48670/moi-00145.
Tsujino, H., Urakawa, S., Nakano, H., Small, R.J., Kim, W.M., Yeager, S.G., Danabasoglu, G., Suzuki, T., Bamber, J.L., Bentsen, M., Böning, C.W., Bozec, A., Chassignet, E.P., Curchitser, E., Boeira Dias, F., Durack, P.J., Griffies, S.M., Harada, Y., Ilicak, M., Josey, S.A., Kobayashi, C., Kobayashi, S., Komuro, Y., Large, W.G., Le Sommer, J., Marsland, S.J., Masina, S., Scheinert, M., Tomita, H., Valdivieso, M., Yamazaki, D., 2018. JRA-55 based surface dataset for driving ocean–sea-ice models (JRA55-do). Ocean Model. 130, 79–139. https://doi.org/10.1016/j.ocemod.2018.07.002.
Untiedt, C.B., Quattrini, A.M., McFadden, C.S., Alderslade, P.A., Pante, E., Burridge, C.P., 2021. Phylogenetic relationships within Chrysogorgia (Alcyonacea: Octocorallia), a morphologically diverse genus of octocoral, revealed using a target enrichment approach. Front. Mar. Sci. 7.
Vancoppenolle, M., Fichefet, T., Goosse, H., Bouillon, S., Madec, G., Maqueda, M.A.M., 2009. Simulating the mass balance and salinity of Arctic and Antarctic sea ice. 1. Model description and validation. Ocean Model. 27, 33–53. https://doi.org/10.1016/j.ocemod.2008.10.005.
Vinogradov, G.M., 2000. Growth rate of the colony of a deep-water gorgonarian Chrysogorgia agassizi: in situ observations. Ophelia 53, 101–103.
Waller, R.G., Goode, S., Tracey, D., Johnstone, J., Mercier, A., 2023. A review of current knowledge on reproductive and larval processes of deep-sea corals. Mar. Biol. 170, 58. https://doi.org/10.1007/s00227-023-04182-8.
Wang, D., Wang, Q., Cai, S., Shang, X., Peng, S., Shu, Y., Xiao, J., Xie, Xiaohui, Zhang, Z., Liu, Z., Lan, J., Chen, D., Xue, H., Wang, G., Gan, J., Xie, Xinong, Zhang, R., Chen, H., Yang, Q., 2019. Advances in research of the mid-deep South China Sea circulation. Sci. China Earth Sci. 62, 1992–2004. https://doi.org/10.1007/s11430-019-9546-3.
Wang, S., Kenchington, E., Wang, Z., Davies, A.J., 2021. Life in the fast lane: modeling the fate of glass sponge larvae in the Gulf Stream. Front. Mar. Sci. 8.
Wang, S., Kenchington, E.L., Wang, Z., Yashayaev, I., Davies, A.J., 2020. 3-D ocean particle tracking modeling reveals extensive vertical movement and downstream interdependence of closed areas in the northwest Atlantic. Sci. Rep. 10, 21421. https://doi.org/10.1038/s41598-020-76617-x.
Wang, S., Murillo, F.J., Kenchington, E., 2022. Climate-change refugia for the Bubblegum coral Paragorgia arborea in the Northwest Atlantic. Front. Mar. Sci. 9.
Watling, L., France, S.C., Pante, E., Simpson, A., 2011. Biology of deep-water octocorals. In: Lesser, M. (Ed.), Advances in Marine Biology. Academic Press, pp. 41–122. https://doi.org/10.1016/B978-0-12-385529-9.00002-0.
Wienberg, C., Beuck, L., Heidkamp, S., Hebbeln, D., Freiwald, A., Pfannkuche, O., Monteys, X., 2008. Franken Mound: facies and biocoenoses on a newly-discovered "carbonate mound" on the western Rockall Bank, NE Atlantic. Facies 54, 1–24. https://doi.org/10.1007/s10347-007-0118-0.
Yahagi, T., Kayama Watanabe, H., Kojima, S., Kano, Y., 2017. Do larvae from deep-sea hydrothermal vents disperse in surface waters? Ecology 98, 1524–1534. https://doi.org/10.1002/ecy.1800.
Young, C.M., He, R., Emlet, R.B., Li, Y., Qian, H., Arellano, S.M., Van Gaest, A., Bennett, K.C., Wolf, M., Smart, T.I., Rice, M.E., 2012. Dispersal of deep-sea larvae from the Intra-American seas: simulations of trajectories using ocean models. Integr. Comp. Biol. 52, 483–496. https://doi.org/10.1093/icb/ics090.
Zalesak, S.T., 1979. Fully multidimensional flux-corrected transport algorithms for fluids. J. Comput. Phys. 31, 335–362. https://doi.org/10.1016/0021-9991(79)90051-2.
Zhai, L., Lu, Y., Higginson, S., Davidson, F., Dupont, F., Roy, F., Chanut, J., Smith, G.C., 2015. High-resolution modeling of the mean flow and meso-scale eddy variability around the Grand Banks of Newfoundland. Ocean Dynam. 65, 877–887. https://doi.org/10.1007/s10236-015-0839-5.
Zhang, Y., Liu, Z., Zhao, Y., Wang, W., Li, J., Xu, J., 2014. Mesoscale eddies transport deep-sea sediments. Sci. Rep. 4, 5937. https://doi.org/10.1038/srep05937.